Technical Report Documentation Page

1. Report No.	2. Government Accession No.	3. Recipient's Catalog No.
SWUTC/10/167274-1		

4. Title and Subtitle	5. Report Date
Towards an Integrated Pavement Design Approach: Using HWTD to Support the MEPDG	November 2010
	6. Performing Organization Code
7. Author(s)	8. Performing Organization Report No.
Sergey Grebenschikov and Jorge A. Prozzi	Report 167274-1
9. Performing Organization Name and Address	10. Work Unit No. (TRAIS)
Center for Transportation Research University of Texas at Austin 1616 Guadalupe Street Austin, TX 78701	11. Contract or Grant No. 10727
12. Sponsoring Agency Name and Address	13. Type of Report and Period Covered
Southwest Region University Transportation Center Texas Transportation Institute Texas A&M University System College Station, TX 77843-3135	14. Sponsoring Agency Code

15. Supplementary Notes

Supported by general revenues from the State of Texas

16. Abstract

Variability of hot-mix asphalt (HMA) production can have drastic effects on pavement performance. A poor gradation or an inappropriate amount of asphalt binder could lead to early distresses and shorter pavement life. Other factors, such as the air void content in the asphalt layer, the type of aggregate gradation used in the mix or volumetrics, in general, can also have significant effects on performance.

This research study focuses on analyzing two techniques for observing the variability of mix production and its effects on pavement performance. First, this study focuses on using the Mechanistic-Empirical Pavement Design Guide (MEPDG) to analyze and predict the effect of the variability of HMA production on rutting in the asphalt layer. Then, this study makes an attempt to compare the results produced by the MEPDG with the results produced by the Hamburg Wheel Tracking Device (HWTD). In order to effectively establish correlations between the two techniques, an experiment was conducted during this research. This experiment focused on using volumetric data from a previous research project. The data from this project was used to model asphalt mixes and pavement structures in the MEPDG and the performance results were then compared to actual data obtained in the laboratory from the Hamburg Wheel Tracking Device (HWTD).

The variability of mix production was captured by analyzing three types of limestone mixes: a coarse dense-graded hot-mix asphalt (Type C, according to TxDOT specification), a fine dense-graded hot-mix asphalt (Type D), and a medium graded stone matrix asphalt (SMA-D). The master gradation band for each mixture was split into three categories: fine, target (actual job mix formula), and coarse. Each mixture was tested at a variable range of binder contents which were obtained using the TxDOT Mix Design Method (TxDOT, 2009). The variability of these mixes and their resistance to rutting as predicted by the MEPDG and measured by the HWTD is discussed in this report.

17. Key Words	18. Distribution Statement
Hot-Mix Asphalt, Asphalt Mix Production, Mechanistic-Empirical Pavement Design Guide (MEPDG), Hamburg Wheel Tracking Device (HWTD)	No restrictions. This document is available to the public through the National Technical Information Service, Springfield, Virginia 22161.

19. Security Classif. (of report)	20. Security Classif. (of this page)	21. No. of pages	22. Price
Unclassified	Unclassified	80	

Form DOT F 1700.7 (8-72) Reproduction of completed page authorized

TOWARDS AN INTEGRATED PAVEMENT DESIGN APPROACH: USING HWTD TO SUPPORT THE MEPDG

by

Sergey Grebenschikov

Jorge A. Prozzi

Research Report SWUTC/10/167274-1

Southwest Region University Transportation Center
Center for Transportation Research
University of Texas at Austin
Austin, Texas 78701

November 2010

DISCLAIMER

The contents of this report reflect the views of the authors, who are responsible for the facts and the accuracy of the information presented herein. This document is disseminated under the sponsorship of the U.S. Department of Transportation, University Transportation Centers Program, in the interest of information exchange. Mention of trade names or commercial products does not constitute endorsement or recommendation for use.

ACKNOWLEDGEMENTS

The authors recognize that support for this research was provided by a grant from the U.S. Department of Transportation, University Transportation Centers Program to the Southwest Region University Transportation Center, which is funded, in part, with general revenue funds from the State of Texas.

ABSTRACT

Variability of hot-mix asphalt (HMA) production can have drastic effects on pavement performance. A poor gradation or an inappropriate amount of asphalt binder could lead to early distresses and shorter pavement life. Other factors, such as the air void content in the asphalt layer, the type of aggregate gradation used in the mix or volumetrics in general, can also have significant effects on performance.

There are several ways to analyze the effects of mix production variability on pavement performance. One way is to create specimens in the laboratory and then subject them to repeated or dynamic mechanical tests (i.e., performance related tests) and quantify their performance based on pre-established criteria. Another way is to use calibrated pavement modeling and analysis tools such as the *Mechanistic-Empirical Pavement Design Guide* (MEPDG).

This research study focuses on analyzing two techniques for observing the variability of mix production and its effects on pavement performance. First, this study focuses on using the Mechanistic-Empirical Pavement Design Guide to analyze and predict the effect of the variability of HMA production on rutting in the asphalt layer. Then, this study makes an attempt to compare the results produced by the MEPDG with the results produced by the Hamburg Wheel Tracking Device (HWTD).

In order to effectively establish correlations between the two techniques, an experiment was conducted during this research. This experiment focused on using volumetric data from a previous research project sponsored by the Texas Department of Transportation (TxDOT). The data from this project was used to model asphalt mixes and pavement structures in the MEPDG and the performance results were then compared to actual data obtained in the laboratory from the Hamburg Wheel Tracking Device (HWTD).

The variability of mix production was captured by analyzing three types of limestone mixes: a coarse, dense-graded hot-mix asphalt (Type C, according to TxDOT specification), a fine dense-graded hot-mix asphalt (Type D), and a medium graded stone matrix asphalt (SMA-D). The master gradation band for each mixture was split into three categories: fine, target (actual job mix formula), and coarse. Coarser mixes tended to be closer to the lower limit of the gradation band while finer mixes tended to be closer to the upper limit of the gradation band. Each mixture was tested at a variable range of binder contents which were obtained using the TxDOT Mix Design Method (TxDOT, 2009). The variability of these mixes and their resistance to rutting as predicted by the MEPDG and measured by the HWTD is discussed in this report.

TABLE OF CONTENTS

LIST OF FIGURES

LIST OF TABLES

EXECUTIVE SUMMARY

In order to assess how well the permanent deformation model embedded in the MEPDG predicts pavement performance, three asphalt mixes were tested in the laboratory using the Hamburg Wheel Tracking Device (HWTD). Thereafter, pavement sections built with the same mixes were modeled using the Design Guide and the results were compared. The data used in this study were obtained from TxDOT's Research Project 0-6045, Laboratory Evaluation of Influence of Operational Tolerance (Acceptance Criterion) on Performance of HMAC. The scope of TxDOT's project was to assess the effect of tolerance limits on pavement performance, yielded this study the opportunity to model pavement sections in the MEPDG using specimen volumetric data obtained from the laboratory.

There were two main objectives to this study. The first objective was to establish correlations between volumetric properties of HMA design and their predicted performance using the MEPDG. The second objective was to compare rutting performance predicted by the MEPDG to rutting performance observed by the Hamburg Wheel Tracking Device.

An experiment was conducted which showed that the permanent deformation model embedded in the MEPDG supports the results from the HWTD. Overall both tests showed that the coarser dense-graded hot-mix asphalt mixture (Type C) performed the best, followed by the fine-dense-graded hot-mix asphalt mixture (Type D), and lastly the stone matrix asphalt mixture (SMA-D). Both, the MEPDG and HWTD results, also showed that for all three mixtures pavement rutting increased as the binder content by weight increases.

These are significant findings because the MEPDG is a relatively new tool available to the pavement engineering community and it is still in its experimental stage. Learning as much as possible about MEPDG and how its performance predictions compares against proven performance-related testing methods such as the Hamburg Wheel Tracking Device is important to highway agencies, contractors, consultant and researchers. It also supports the use of the HWTD for mix design as it is done in Texas.

This research report discusses the MEPDG's permanent deformation model and how its ability to predict pavement rutting compares to the HWTD test results. The report briefly introduces the MEPDG and the HWTD. Then, it identifies the procedures for data collection, data implementation, and data analysis. Lastly, it discusses the results of the study and draws the most significant conclusions from the research.

CHAPTER 1 - INTRODUCTION

There are several known methods for estimating the offset and development of pavement distresses such as surface rutting. Over the years, simple calculations based on the volumetric properties of the hot-asphalt mixture have served as reasonable indicators of the types of distresses a pavement could develop. Another popular method of predicting pavement distresses has been through the application of performance-related tests. Typically, performance-related tests subject a laboratory specimen to a static, repeated or dynamic loading pattern and record the specimen's response and performance until it reaches pre-established failure criteria. There are many types of performance-related tests that measure a variety of pavement responses. Some are simple such as the static creep test which applies a load on a specimen and records the specimen's deformation with time under controlled temperature conditions. Others are more complex and require expensive laboratory equipment, such as the rolling wheel tests. The Hamburg Wheel Tracking Device (HWTD) is one such piece of equipment. It is commonly used in Texas to establish the potential of the asphalt mixture to resist permanent deformation and moisture damage, i.e. stripping.

1.1. Hamburg Wheel Tracking Device (HWTD)

The Hamburg Wheel Tracking Device was developed in Hamburg, Germany by Helmut-Wind Incorporated and can be observed in Figure 1.1 (Prozzi, Aguiar-Moya, Smit, Tahmoressi, and Fults, 2006).

Figure 1.1 Hamburg Wheel Tracking Device (courtesy of FHWA)

The HWTD is an electrically powered machine that tests rutting and moisture susceptibility of hot-mix asphalt (HMA) (AASHTO 2006). Typically, a laboratory compacted HMA specimen or a core taken from the field is repetitively loaded using a reciprocating steel wheel while the specimen is submerged in a temperature controlled water bath. The deformation in the wheel path is measured by a linearly-variable differential transducer (LVDT) as the wheel

moves over the specimen. The HWTD measures rut depth as a function of wheel passes (TxDOT, Tex-242-F). This test is popular for determining premature failure susceptibility of asphalt mixtures because it is relatively simple to conduct and it provides results that are comparable to field performance (Yildirim and Stokoe II, 2006).

In Texas, the test is currently being performed on cylindrical specimens with a 6 in. (150 mm) diameter and a 2.4 ± 0.1 in. (62 ± 2mm) specimen height. The cylindrical specimens are compacted with a Superpave Gyratory Compactor (SGC) to a density of 93 ± 1% prior to testing. Testing is conducted under water at 122 ± 2°F (50 ± 1°C). Two specimens are typically cut and fitted together in a mold (as seen on Figure 1.2) and placed inside the machine. Loading is accomplished by applying a force of 158 ± 5 lbs. (705 ± 22 N) onto a steel wheel with a diameter of 8 in. (203.6 mm) and a width of 1.85 in. (47 mm). The steel wheel is then tracked back and forth over the two cylindrical test samples. Test samples are loaded to 20,000 wheel passes or until a deformation of 12.5 mm is reached.

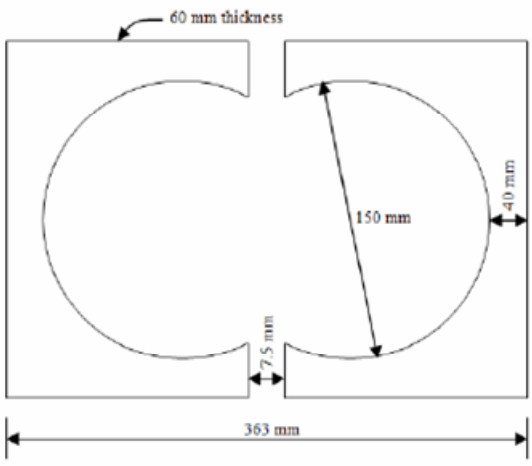

Figure 1.2 Test specimen mold for the HWTD

1.2. Mechanistic-Empirical Pavement Design Guide (MEPDG)

A rather new concept for assessing pavement performance is through the use of computer integrated modeling and analysis tools (Huang, 2004). These tools are computer software programs that attempt to model relationships between material properties, such as pavement response to specific traffic loading and environmental conditions. Then, using those relationships they attempt to quantify pavement performance. One such modeling tool is the recently developed Mechanistic-Empirical Pavement Design Guide or MEPDG.

The Mechanistic-Empirical Pavement Design Guide is a joint effort by the American Association of State Highway and Transportation Official's (AASHTO) Joint Task Force on Pavements, the National Cooperative Highway Research Program (NCHRP), and the Federal Highway Administration (FHWA) to bring researchers and pavement engineers a state-of-the-art tool for designing pavement structures and analyzing pavement performance (AASHTO, 2008).

As the name implies, the MEPDG combines both mechanistic principles and empirical models to predict pavement performance. The design guide allows the user to model the structure of a pavement section and then subject it to theoretical traffic loads under various climate conditions. The MEPDG then calculates the response and the distresses developed in the pavement for a certain design period.

Each distress type (i.e. fatigue cracking, thermal cracking, rutting, or roughness) predicted by the MEPDG has a structural response model associated with it that is embedded inside the program. The structural response model calculates mechanical responses such as deflections, stresses and strains experienced by the pavement section when subjected to a traffic load. For rutting, the structural response model embedded in the MEPDG is based upon the elastic layer theory and is computed by a multi-layer linear elastic software program called JULEA (AASHTO, 2008). In order to use JULEA to calculate mechanical responses, it is necessary to determine the dynamic modulus of the mixture or E*. The design guide employs the following equation to predict the dynamic modulus over a range of temperatures, rates of loading, and aging conditions (NCHRP, 2004):

Equation 1.1 Final recommended dynamic modulus predictive equation.

$$\log E^* = 3.750063 + 0.02932\,\rho_{200} - 0.001767\,(\rho_{200})^2 - 0.002841\,\rho_4 - 0.058097\,V_a - 0.802208\left(\frac{V_{beff}}{V_{beff} + V_a}\right) + \frac{3.871977 - 0.0021\,\rho_4 + 0.003958\,\rho_{38} - 0.000017\,(p_{38})^2 + 0.005470\,\rho_{34}}{1 + e^{(-0.603313 - 0.313351\,\log(f) - 0.393532\,\log(\eta))}}$$

where:

E*	=	dynamic modulus, psi
η	=	bitumen viscosity, 10^6 Poise
f	=	loading frequency, Hz.
V_a	=	air void content, %
V_{beff}	=	effective bitumen content, % by volume
ρ_{34}	=	cumulative % retained on ¾ in sieve
ρ_{38}	=	cumulative % retained on 3/8 in sieve
ρ_4	=	cumulative % retained on the No. 4 sieve
ρ_{200}	=	% passing the No. 200 sieve

This prediction equation depends heavily upon mixture volumetric properties such as the air voids content, the effective binder content and the aggregate gradation of the mixture (NCHRP, 2004). Based on the dynamic modulus (E*) obtained from this equation and based on the traffic loading and weather conditions, the MEPDG uses JULEA to compute the mechanical responses developed in each layer of the structure.

The MEPDG then converts the mechanical responses (deflections, stresses and strains) calculated by the structural response model into expected pavement distresses by the application of distress prediction equations or transfer functions. In general, transfer functions are derived

from material performance under laboratory testing conditions; therefore, a shift factor is then applied. For rutting, the rate of accumulation of plastic deformation is measured in the laboratory using a repeated load permanent deformation tri-axial test. This test applies pulse loads on a specimen to develop a relationship between the plastic strain in the specimen and its permanent deformation. That relationship is then used to develop a transfer function. For rutting in the asphalt concrete layer, the MEPDG currently employs the following transfer function (AASHTO, 2008).

Equation 1.2 Distress prediction equation used to predict rutting in the AC Layer

$$\Delta_{p(HMA)} = \varepsilon_{p(HMA)} h_{HMA} = \beta_{1r} \kappa_z \varepsilon_{r(HMA)} 10^{k1r} N^{k2r\beta 2r} T^{k3r\beta 3r}$$

where:

$\Delta_{p(HMA)}$ = Accumulated permanent vertical deformation in the HMA layer (in.),
$\varepsilon_{p(HMA)}$ = Accumulated permanent axial strain in the HMA layer (in./in.),
$\varepsilon_{r(HMA)}$ = Elastic strain calculated by the structural response model at mid-depth of each HMA layer (in.),
h_{HMA} = Thickness of the HMA layer/sublayer (in.),
N = Number of axle load repetitions
T = Mix or pavement temperature (°F),
κ_z = Depth confinement factor
k1r,2r,3r = Global field calibration factors
β1r,2r,3r = Local or mixture field calibration factors

$$\kappa_z = (C_1 + C_2 * depth) * 0.328196^{depth}$$

$$C_1 = -0.1039 * H^2_{ac} + 2.4868 * H_{ac} - 17.342$$

$$C_2 = 0.0172 * H^2_{ac} - 1.7331 * H_{ac} + 27.428$$

where:

D = Depth below the surface (in.),
H_{ac} = Total HMA thickness (in.)

From this distress prediction equation it can be observed that the MEPDG predicts pavement rutting based on a relationship between elastic strains and plastic strains in the asphalt pavement layers. The deformations predicted by this transfer function are then accumulated to calculate permanent deformation over the design life. From the right side of the equation it can be seen that permanent deformation is further adjusted by calibration factors. The term 'calibration' refers to a mathematical process of minimizing the difference in error between observed and predicted values (NCHRP, 2003). In order to reduce error and make predictions more robust, the transfer functions embedded into the MEPDG have been calibrated with field performance data obtained from the Long Term Pavement Performance (LTPP) Database (http://www.ltpp-products.com/).

The approach utilized in the MEPDG to estimate pavement performance is based upon an incremental damage approach. The design guide breaks up a pavement's life into one-month time intervals. Then, using the distress prediction equations it attempts to convert the mechanical responses of the pavement (engendered by conceptual traffic loads and weather conditions) into incremental distress. Then the design guide quantifies these distress types for a single time interval. The overall pavement performance is measured by summing up the distresses in each one of these time intervals for the entire life of the structure.

In principle, pavement performance predicted by the MEPDG should show similar trends to the performance obtained from the repeated load tri-axial test because the equation used to calculate the accumulated permanent deformation is derived directly from strain relationships observed through the repeated load tri-axial test. Therefore, if for a certain mix with set aggregate properties and volumetric data, the laboratory test showed that rutting resistance was better for a finer gradation than for a coarser gradation, the results from the MEPDG should reflect similar trends. If such is the case, then it would be beneficial to explore how pavement rutting predicted by the MEPDG compares to rutting of the mixture observed by laboratory tests such as the Hamburg Wheel Tracking Device (HWTD).

CHAPTER 2-EXPERIMENTAL DESIGN

The experiment conducted as part of this study was based upon data collected as part of TxDOT Research Project 0-6045. To assess the effect of current operational tolerances on pavement performance, this project investigated several material components of asphalt concrete pavements. Specifically, the research project evaluated the effect of aggregate type (limestone and siliceous gravel), aggregate gradation, maximum aggregate size, and asphalt binder content by weight. The goal of the project was to observe how changing these properties within current operational tolerances affected the performance of the mixes in the laboratory. This was accomplished by making asphalt concrete specimens in the lab, and then testing their performance under the Bending Beam Fatigue Test *(*AASHTO T321-03) the Overlay Test (TXDOT, Tex-248-F), and the Hamburg Wheel Tracking Device (TxDOT, Tex-242-F). The following sections focus on the data which was used for the experiment described in this report.

2.1. Mixture Design

The experiment reported here was based upon three limestone mixtures: coarse dense-graded hot-mix asphalt (Type C), fine dense-graded hot-mix asphalt (Type D), and gap-graded stone matrix asphalt (SMA-D). These mixtures were blended to meet aggregate quality and gradation requirements discussed under "Dense-Graded Hot-Mix Asphalt" (Item 341) and "Stone Matrix Asphalt" (Item 346) of the 2004 *TxDOT Standard Specifications for Construction and Maintenance of Highways, Streets, and Bridges*. Furthermore, the master gradation bands for each mixture specify a minimum and a maximum percentage of aggregates allowed to pass through certain sieve sizes (gradation envelope). Therefore, it was important to obtain a job mix formula (JMF) well within the envelope, so as the tolerance limits were applied, the mix remained inside specifications. Each mixture, then, was mixed at three different gradation levels that were labeled as: fine, target (as per JMF), and coarse. Coarser mixes tended to be closer to the lower limit as allowed by current tolerances, while finer mixes tended to be closer to the upper limit of the tolerances.

Tables 2.1 and 2.2 show how aggregates from different stockpiles were blended to capture the tolerances within the master gradation band for the coarse-dense-graded hot-mix asphalt mixture (Type C).

Table 2.1 Aggregate Blending for Type C Limestone Mixture

Aggregate Stockpile	Percentage by weight		
	Target Gradation	Fine Gradation	Coarse Gradation
Delta C-Rock	25.0%	21.0%	25.0%
Centex D-Rock	18.0%	18.0%	23.0%
Centex F-Rock	23.0%	23.0%	18.0%
Centex Manufactured Sand	26.0%	30.0%	26.0%
Travis Field Sand	8.0%	8.0%	8.0%

Table 2.2 Gradation for Type C Limestone Mixture

Sieve Size		Cumulative Percentage Passing by Weight				
US-Standard	Metric-Standard	Target Gradation	Fine Gradation	Coarse Gradation	Specification Lower Limit	Specification Upper Limit
3/4"	19.0mm	99.7	99.7	99.7	95.0	100.0
3/8”	9.5mm	70.3	74.2	68.9	70.0	85.0
#4	4.75mm	53.3	57.3	49.7	43.0	63.0
#8	2.36mm	37.4	41.1	36.5	32.0	44.0
#30	0.60mm	18.5	20.1	18.4	14.0	28.0
#50	0.30mm	11.9	12.6	11.8	7.0	21.0
#200	0.075mm	3.6	3.7	3.6	2.0	7.0

These chosen aggregate blends are also shown in Figure 2.1 below, where the dotted lines represent the upper and lower boundaries of the gradation band of TxDOT specification for this mix type.

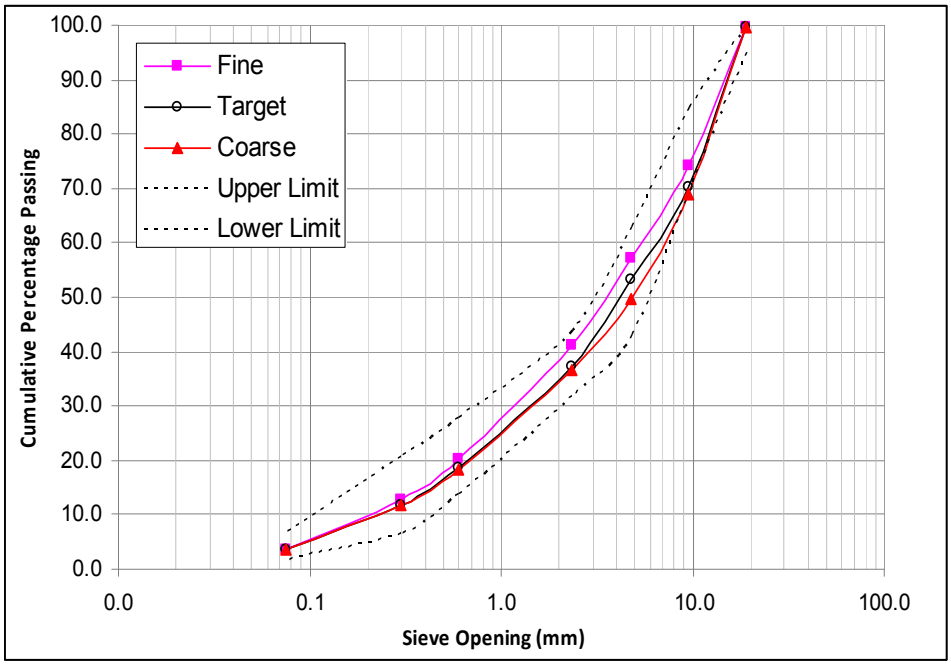

Figure 2.1 Master gradation band for Type C limestone mixture

For the finer dense-graded hot-mix asphalt mixture (Type D), a different approach was taken. First, the gradation for the target level was defined, and then the individual percentages retained in specific sieves were either increased or decreased to achieve the desired gradation level. This allowed the researcher to produce the finer and coarser mixes that were allowed within the current operational tolerances. Tables 2.3 and 2.4 show how aggregates from different stockpiles were blended to achieve the target gradation and then adjusted to capture the tolerances within the master gradation band.

Table 2.3 Aggregate Blending for Type D Limestone Mixture

Aggregate Stockpile	Percentage by Weight
Delta Grade 4	28%
Centex D-Rock	20%
Centex F-Rock	15%
Centex Man Sand	29%
Travis Field Sand	8%

Table 2.4 Gradation for Type D Limestone Mixture

Sieve Size		Cumulative Percentage Passing by Weight				
US-Standard	Metric-Standard	Target Gradation	Fine Gradation	Coarse Gradation	Specification Lower Limit	Specification Upper Limit
1/2"	12.5mm	97.9	100.0	92.9	98.0	100.0
3/8"	9.5mm	79.3	84.3	74.3	85.0	100.0
#4	4.75mm	48.5	53.5	43.5	50.0	70.0
#8	2.36mm	36.9	39.9	33.9	35.0	46.0
#30	0.60mm	19.4	22.4	16.4	15.0	29.0
#50	0.30mm	12.0	15.0	9.0	7.0	20.0
#200	0.075mm	2.7	4.7	2.0	2.0	7.0

The master gradation band for Type D mix is also plotted in Figure 2.2 below, where the dotted lines are the upper and lower boundaries of the gradation band.

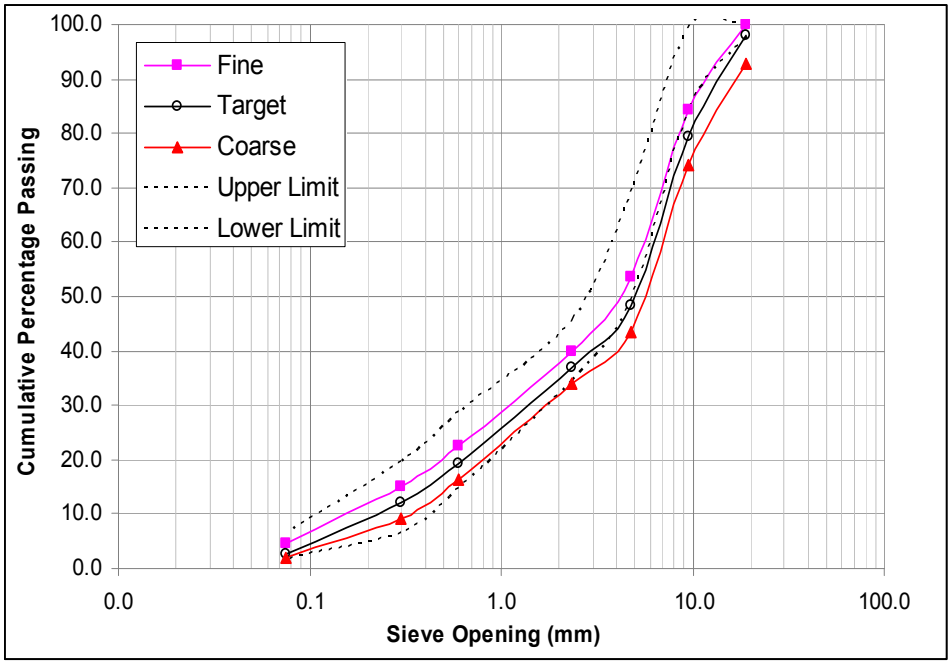

Figure 2.2 Master gradation band for Type D limestone mixture

For the stone matrix asphalt mixture (SMA-D), aggregates from different stockpiles were blended to achieve three gradations that capture the tolerances within the master gradation band. These results are shown in Tables 2.5 and 2.6.

Table 2.5 Aggregate Blending for SMA Limestone Mixture Type D

Aggregate Stockpile	Percentage by weight		
	Target Gradation	Fine Gradation	Coarse Gradation
Delta C-Rock	39.5%	35.0%	44.8%
Centex D-Rock	41.2%	40.8%	40.8%
Centex F-Rock	0.0%	0.0%	1.3%
Dry Screening	15.0%	20.3%	6.8%
Fly Ash	4.0%	3.5%	6.0%
Cellulose Fiber	0.3%	0.3%	0.3%

Table 2.6 Gradation for SMA Limestone Mixture Type D

Sieve Size		Cumulative Percentage Passing by Weight				
US-Standard	Metric-Standard	Target Gradation	Fine Gradation	Coarse Gradation	Specification Lower Limit	Specification Upper Limit
3/4"	19.0 mm	100.0%	100.0%	100.0%	100.0%	100.0%
1/2"	12.5 mm	88.0%	93.0%	83.0%	85.0%	99.0%
3/8"	9.5 mm	53.0%	58.0%	48.0%	50.0%	75.0%
#4	4.75 mm	25.0%	30.0%	20.0%	20.0%	32.0%
#8	2.36 mm	18.0%	23.0%	13.0%	16.0%	28.0%
#16	1.18 mm	15.6%	18.6%	12.6%	8.0%	28.0%
#30	0.60 mm	13.7%	16.7%	10.7%	8.0%	28.0%
#50	0.30 mm	12.1%	15.1%	9.1%	8.0%	28.0%
#200	0.075 mm	8.2%	10.2%	8.0%	8.0%	12.0%

The master gradation band for the SMA-D mix is also shown in Figure 2.3, where the dotted lines are the upper and lower boundaries of the gradation band.

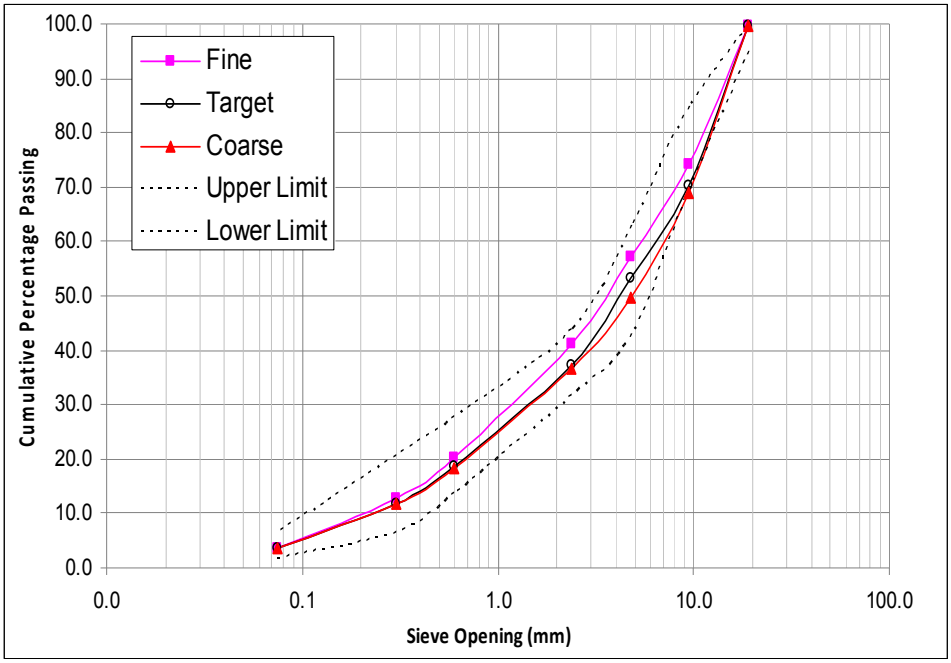

Figure 2.3 Master gradation band for SMA-D limestone mixture

For each mixture type and the corresponding three gradations, the optimum asphalt content (OAC) was determined. This was determined in accordance with TXDOT's Tex-204-F *Design of Bituminous Mixes* test procedure. For mixture Type C the optimum asphalt content was determined to be 4.6% by mass, for mixture Type D it was 5.3% and for mixture Type SMA-D it was at 6.2%. Based on the OAC, four binder contents were selected around the OAC for the dense graded mixes and three binder contents for the stone matrix asphalt mix. Based on this selection, the following 33 combinations were prepared in the lab.

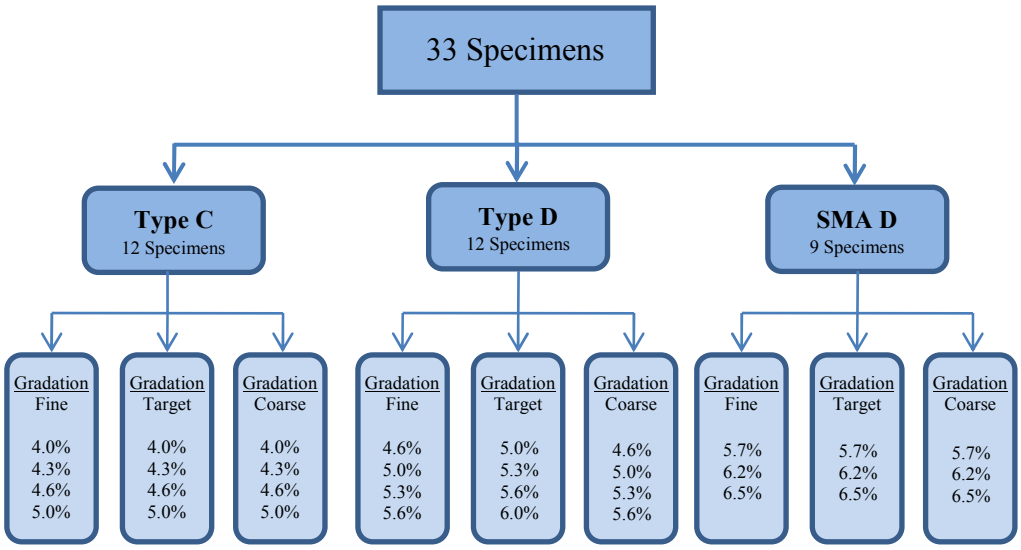

Figure 2. 4 Tree diagram categorizing combinations used in the experiment

2.2. Modeling of Sections in the MEPDG

Based on the criteria shown in Figure 2.4, 33 specimen combinations were prepared in the laboratory. Each combination was compacted to a density of 93% ± 1% (TXDOT, Tex-242-F) with the Superpave Gyratory Compactor and tested using the Hamburg Wheel Tracking Device. The densities of the compacted specimens and the maximum theoretical density (G_{mm}) of each batch were used to determine all volumetric properties necessary to model the tested mixes on a typical pavement using the MEPDG. In order to model the mixes using MEPDG, the following volumetric data were required from each combination in Figure 2.4:

- Percent air voids
- Effective binder content
- Specimen unit weight

These volumetric data were calculated for each combination using "Asphalt Concrete Mix Design" procedures from *Materials for Civil and Construction Engineers* (Mamlouk & Zaniewski, 2006). The volumetric properties were calculated with two major constraints:

1. Aggregate absorption was not measured but was assumed to be 1.5% based on historical data for the given aggregate source. Hence, the percent by volume of absorbed binder was also assumed to be 1.5%.

2. Some of the work was outsourced to PaveTex Engineering and Testing, Inc. (www.pavetex.com) whose task was to compact the specimens to an appropriate density and test them with the HWTD. The exact densities to which each specimen was compacted is not known. Therefore a sensitivity analysis had to be conducted where every specimen which was tested with the HWTD was also modeled with the MEPDG at three air void contents (6%, 7% and 8%) to cover the allowable density range of 93% ± 1%.

The volumetric data for all the specimens modeled in the MEPDG can be found in Appendix C.

Before an analysis using the MEPDG could be conducted, certain criteria had to be established within the design guide to make sure there was consistency between the testing procedure and the modeling. Location, traffic characteristics, climate, material characterization, and failure criteria of the distress in question had to be considered.

Since the study was conducted with aggregate blends and a binder type that are commonly used in Texas, it was appropriate to choose a location for the analysis that was also in Texas. The city of El Paso was chosen as the site for the analysis, mainly because of the availability of traffic information in the region obtained from the LTPP database from an earlier study (Banerjee, Aguiar-Moya, Prozzi, 2008). Information such as vehicle class distribution and traffic growth rate was obtained from the LTPP database and input into the design guide. Other information, such as monthly adjustment factors and hourly distribution factors which were unknown, were left at the design guide's default setting.

Climatic data for the analysis was generated by interpolating data from several weather stations located near El Paso using the Enhanced Integrated Climatic Model (EICM) tool embedded in the MEPDG. A three layer system was chosen with a semi-infinite subgrade, an 8.4" granular base consisting of crushed stone, and a 6" HMA concrete layer. The input level for strength properties for both the base and the subgrade were set to Level 3 or the "best estimated" default values given by the MEPDG. The input level for asphalt material properties was set to Level 2, which allowed for the adjustment of volumetric data of the asphalt layer, the aggregate gradation of the asphalt mix, and the binder type to represent the material tested in the laboratory.

To carry out the comparative analysis, the distress chosen was the permanent deformation (or rutting) in the asphalt concrete layer, and the failure criteria was defined as 0.25" of maximum mean rut depth in the wheel path (AASHTO, 2008). The design/analysis period was set to 20 years, and the design reliability of the project was set to 90%. To remain consistent, calibration factors for all distress prediction equations were left at the national calibration level for the analysis. The binder type used in the project was a polymer modified PG76-22S with a specific gravity of 1.03. Since the MEPDG does not account for the specific polymer used, a

PG76-22 binder was used for the analysis. Table 2.7 presents a summary of the basic design criteria that were selected and held constant throughout the experiment.

Table 2.7 Design Criteria Established and Held Constant Throughout the Analysis

Binder Type	PG76-22S
SG_{BINDER} (G_b)	1.03
Location	El Paso
Design Life	20 years
Reliability	0.90
AC Rutting, mean depth	0.25"
Calibration Factors	National
Initial AADTT	500
Traffic Growth Rate	5.5%, Linear
Structure	**Thickness**
HMA Layer	6.0"
Base	8.4"
Subgrade	Semi-infinite

CHAPTER 3-ANALYSIS OF DATA

The MEPDG and the Hamburg Wheel Tracking Device, although conceptually very different, can be used to assess the rutting potential of a hot-mix asphalt layer. Both capture the accumulated deformation of the asphalt mixture as a function of the number of wheel or axle passes. In order to effectively understand the results from the two testing methods, proper data analysis techniques and procedures must be identified. This section of the report discusses the techniques necessary for analyzing the results gathered from the HWTD and the MEPDG so they can be compared.

3.1. Analysis Techniques for HWTD

The Hamburg Wheel Tracking Device measures the deformation of the asphalt specimens at 11 points along the wheel path. Figure 3.1 shows an approximate location of these points.

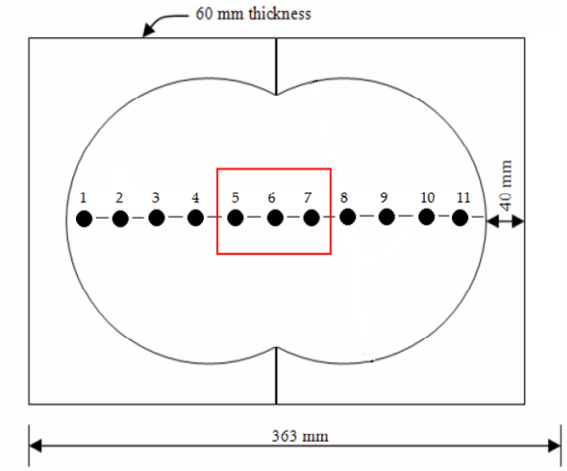

Figure 3.1 Points at which deformation is measured by the HWTD

Naturally, the deformation measured along the specimen mold presents a lot of variability. Points 1 and 11 for example, typically experience more deformation than the rest due to chipping of the aggregate from the specimen at the edge of the mold. Points 2, 3, 4 and 8, 9, 10 give the most consistent results as they measure the deformation in the middle of each specimen. Ideally, for a robust analysis of specimen rutting, these points would be the points used in the calculation of the deformation. Current testing specifications, however, indicate that the test results should be reported by taking the average deformation at the center of the two joint specimens. Therefore, points 5, 6, and 7 were selected for the analysis. Points 5, 6, and 7 are highlighted in Figure 3.1.

Another problem which posed a concern was the sensitivity of the LVDT devices to measurements of deformation in the wheel path as the wheel moved along the mold. Due to the

sensitivity of the devices, the test results captured a significant amount of noise in the data. To reduce the amount of noise measured at points 5, 6, and 7, a lower bound average value was used to evaluate deformation for each specimen. This technique made the most logical sense because it reduced variability by minimizing outliers within the dataset which would have otherwise skewed the overall results. This approach is also consistent with current TxDOT testing specifications. The median was also considered for the analyses of HWTD data because it is typically the more robust value. However, it was not chosen due to the high sensitivity of the deformation data obtained from the LVDT device.

The results obtained from the HWTD consisted of rut depth, creep slope, stripping inflection point, and stripping slope, as seen in Figure 3.2. One good way of analyzing the data produced by the HWTD test is to directly observe the rut depth of each specimen at a specified number of wheel passes. The rut depth for each specimen was recorded at 10,000, 15,000, and 20,000 wheel passes. Deformation at this number of wheel passes can be found in Appendix E for all specimens tested.

Another good method is looking at the creep slope of each specimen. The creep slope, which is the inverse of deformation rate within the linear region of the deformation curve after post-compaction and prior to stripping, is a good indicator of pavement performance (Prozzi, Aguiar-Moya, Smit, Tahmoressi, and Fults, 2006). Flatter slopes tend to represent higher resistance to pavement rutting while angled slopes tend to represent less resistance.

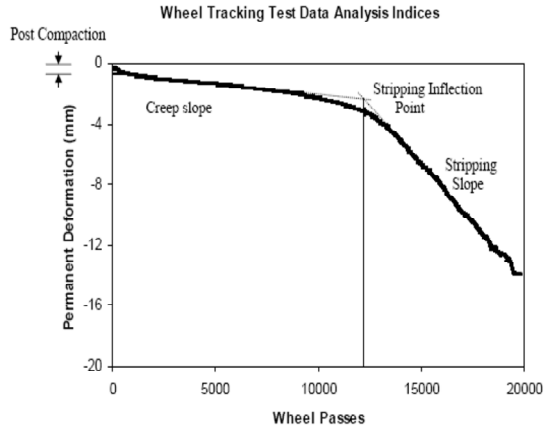

Figure 3.2 Definition of results from HWTD (after Brown et al., 2001b)

Pavement performance in this experiment was assessed using both techniques. First, rut depth data from the HWTD analysis was grouped by mixture type, and the performance of each specimen was plotted based on the gradation and the binder content by weight. Then the creep slope for each specimen was determined. The objective of this analysis was to observe the effects of gradation and binder content on specimen rutting under the HWTD. Stratifying specimens by groups allowed for comparison of the mixtures to see which yielded the best results.

3.2. Analysis Techniques for MEPDG

The MEPDG calculates pavement distresses through an incremental damage approach. For pavement rutting, it calculates the maximum mean rut depth in the asphalt concrete (AC) layer at every one-month time interval and accumulates it over the entire design life of a pavement. The traffic loading experienced during each one-month time interval is a function of annual average daily truck traffic (AADTT) that is adopted from the truck class distribution spectrum, and the axle load distribution spectrum. Plotting the 240[1] performance data points for each modeled pavement could become time-consuming and confusing, so the performance data plots presented in Chapter 4 show only nine time points. Because significant pavement rutting occurs during the initial months after construction, the data points plotted have to effectively capture the initial rutting, as well as accumulated rutting from there forth. So, critical data points for the analysis were selected to be at 1, 3, 6, 12, 36, 60, 120, 180, and 240 months after construction. The maximum mean rut depth for these time intervals as predicted by the MEPDG can be found in Appendix D.

To analyze the results from the MEPDG, various volumetric properties such as the effective binder content by volume, voids in the mineral aggregate (VMA), and voids filled with asphalt (VFA), were plotted against AC layer rutting after 240 months (20 years). It has been established that these volumetric parameters play a significant role in overall pavement rutting, and it was important to develop a better understanding of how these parameters affect the distress prediction models imbedded within the MEPDG.

To compare the integrity of the design guide's prediction models, rut depth in the AC layer predicted by the MEPDG was also compared against rut depth data measured by the HWTD. The testing results were once again grouped by mixture type and a simple comparison was made where rut depth was plotted against the life cycle of the test (i.e. 240 months in the case of MEPDG and 20,000 wheel passes in the case of the HWTD).

[1] A design life of 20 years= 240 months=240 time points

CHAPTER 4-RESULTS

This section of the report presents the results obtained from the laboratory experiment, the MEPDG simulations and their comparisons. The objective of this report was to use the Mechanistic-Empirical Pavement Design Guide to analyze and predict the variability of mix production on rutting in the asphalt layer. Then, it was to compare the results produced by the MEPDG with the results produced by the Hamburg Wheel Tracking Device. The first part of this section presents results from the MEPDG and the second part presents results from the HWTD and compares them to results from the MEPDG.

4.1. MEPDG RESULTS

The results produced from the performance analysis conducted by the MEPDG revealed interesting correlations between pavement rutting and each mix's respective volumetric properties. Certain trends between pavement rutting and specimen gradation, effective binder content, VMA, and VFA that were observed are presented below.

4.1.1. Effective Binder Content vs. Rutting

Figure 4.1 below shows the relationship between effective binder content by volume and pavement rutting in the asphalt layer after 20 years of analysis for each one of the three mixes: Type C, Type D and SMA-D (Figures 4.1a, 4.1b and 4.1c, respectively). For each of these mixes, these plots show two main effects.

1. The effect of different gradations (fine, target, and coarse) within each mixture's gradation band on AC rutting.
2. The mixtures' sensitivity to density (air voids) and its effects on rutting of the asphalt layer.

For each of the gradation types (target, fine and coarse) and for each binder content by weight, three markers can be observed. These markers correspond to 92, 93 and 94% relative density.

(a)

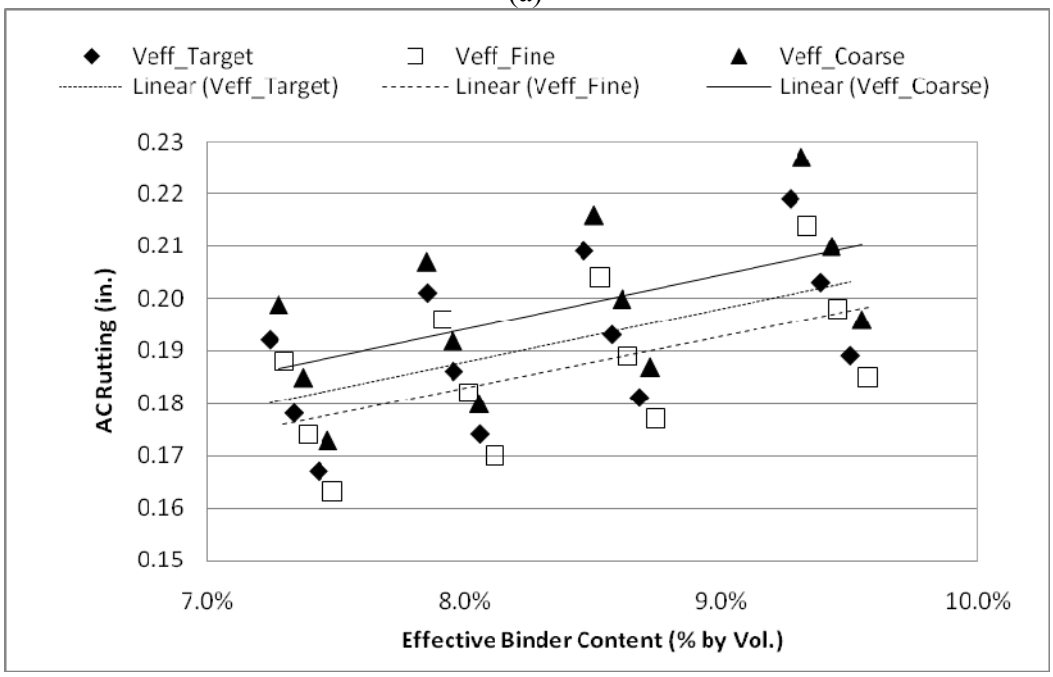
Veff_Target
Veff_Fine
Veff_Coarse
Linear (Veff_Target)
Linear (Veff_Fine)
Linear (Veff_Coarse)
AC Rutting (in.)
0.23
0.22
0.21
0.20
0.19
0.18
0.17
0.16
0.15
7.0%
8.0%
9.0%
10.0%
Effective Binder Content (% by Vol.)

(b)

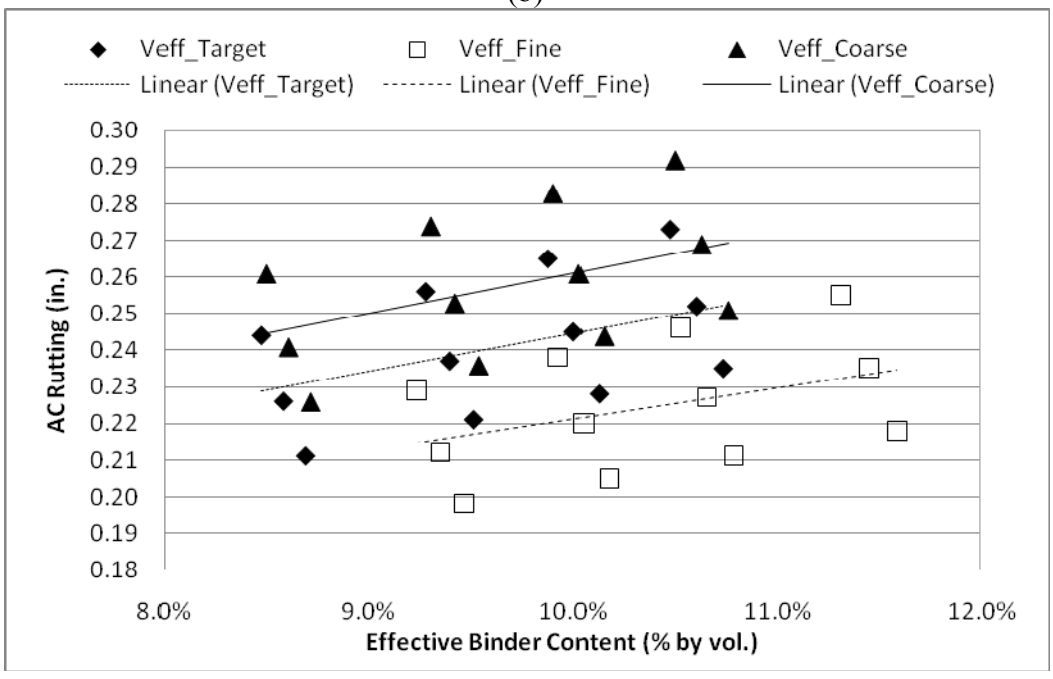
Veff_Target
Veff_Fine
Veff_Coarse
Linear (Veff_Target)
Linear (Veff_Fine)
Linear (Veff_Coarse)
AC Rutting (in.)
0.30
0.29
0.28
0.27
0.26
0.25
0.24
0.23
0.22
0.21
0.20
0.19
0.18
8.0%
9.0%
10.0%
11.0%
12.0%
Effective Binder Content (% by vol.)

(c)

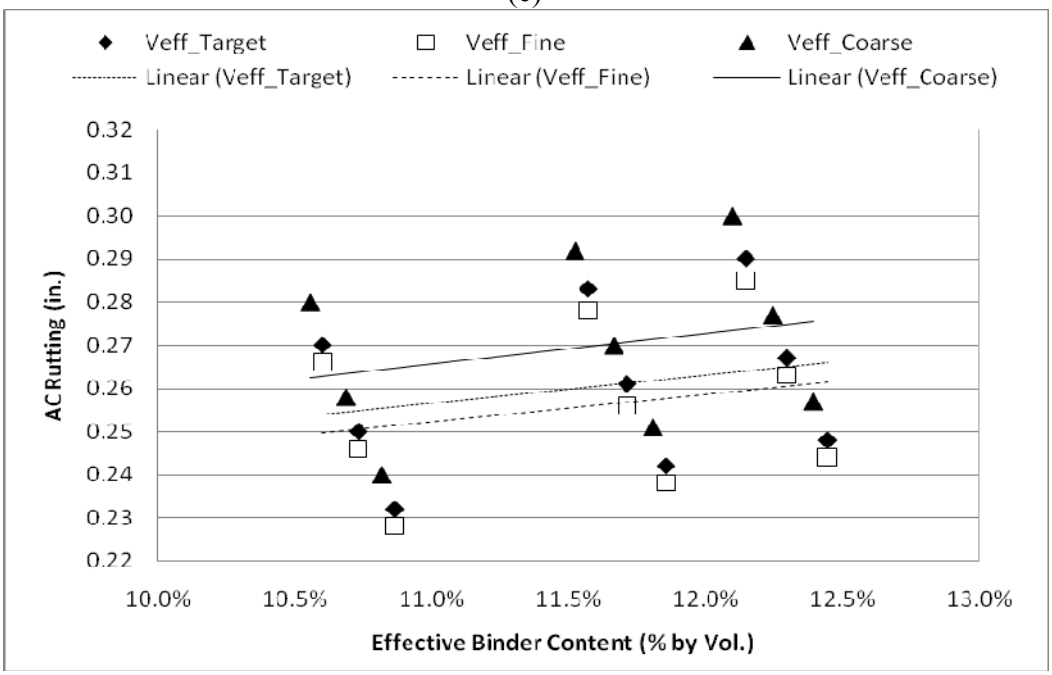

Figure 4.1 Effective binder content vs. AC rutting
for *(a)* Types C, *(b)* D, and *(c)* SMA D

For all three mixture (Type C, Type D, and SMA-D), pavement rutting was observed to increase as the effective asphalt binder content by volume increases. Also, it can be observed that for all three mixtures types, pavement with mixes that were on the finer side of the target gradation tended to have a better performance (less rutting) relative to target and coarser mixes. It was also noted that pavement sections whose mixes were modeled to 94% relative density (or 6% air voids content) performed better than pavement sections that were modeled to 93% density or to 92% density. For the Type C mixture, sections compacted to 92% density experienced on average 7.9% more asphalt rutting than those compacted to 94% density. For the Type D mix, there was an 8.3% difference between the results, and for the stone matrix asphalt mixture (SMA-D) there was an 8.4% difference between the results.

4.1.2. Voids in Mineral Aggregate (VMA) vs. Rutting

To attain a more fundamental understanding of how the effective asphalt binder content and the air void content of specimens interact together to effect pavement performance, voids in the mineral aggregate (VMA) were plotted against rutting in the asphalt layer. These results are shown in Figures 4.2a, 4.2b and 4.2c for Type C, Type D and SMA-D, respectively. From the plots in Figures 4.2, it can be seen that for all limestone mixes, pavement rutting in the asphalt layer increased as VMA increased. These figures also give a better perspective on how the various gradations within each mixture's master gradation band (i.e. fine, target, and coarse) effect the overall rutting in the asphalt layer for different VMA.

For all three mixes, it was observed that those pavement sections modeled with the asphalt properties on the finer side of the target gradation tended to experience less rutting than those sections on the coarser side. For example, with Type C the sections modeled on the coarser side, on average, experienced 5.9% more rutting than those modeled on the finer side of the target gradation. The Type D mixture experienced a 14.7% increase in asphalt rutting going from a finer to a coarser gradation, while for the SMA-D mixture, the increase in rutting from finer to coarser was in the order of 5.2%.

(a)

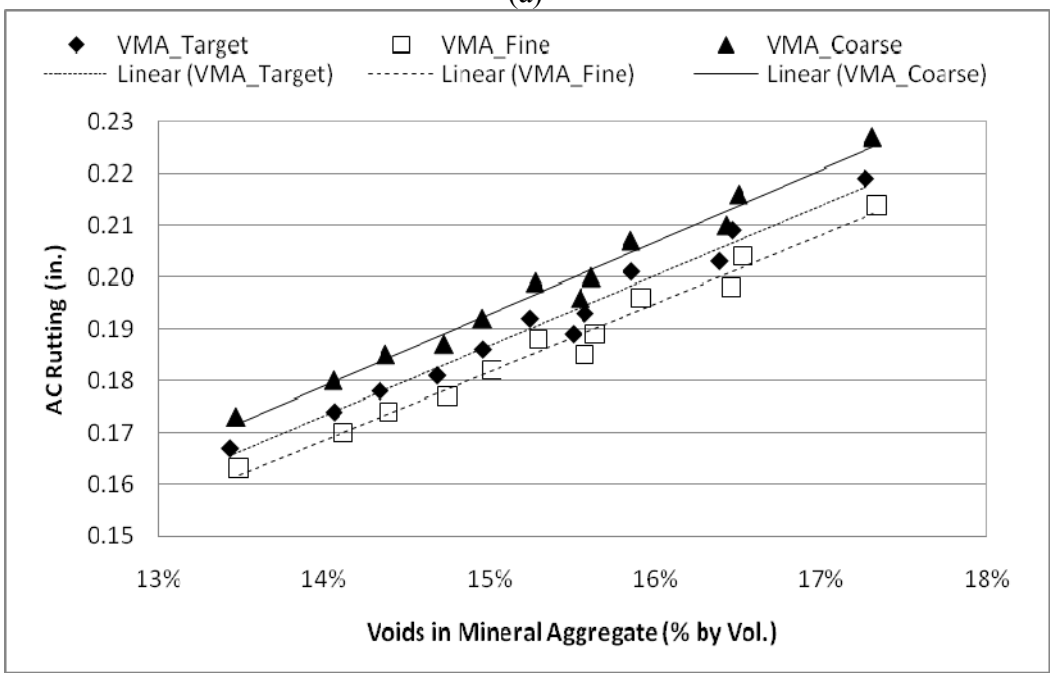

(b)

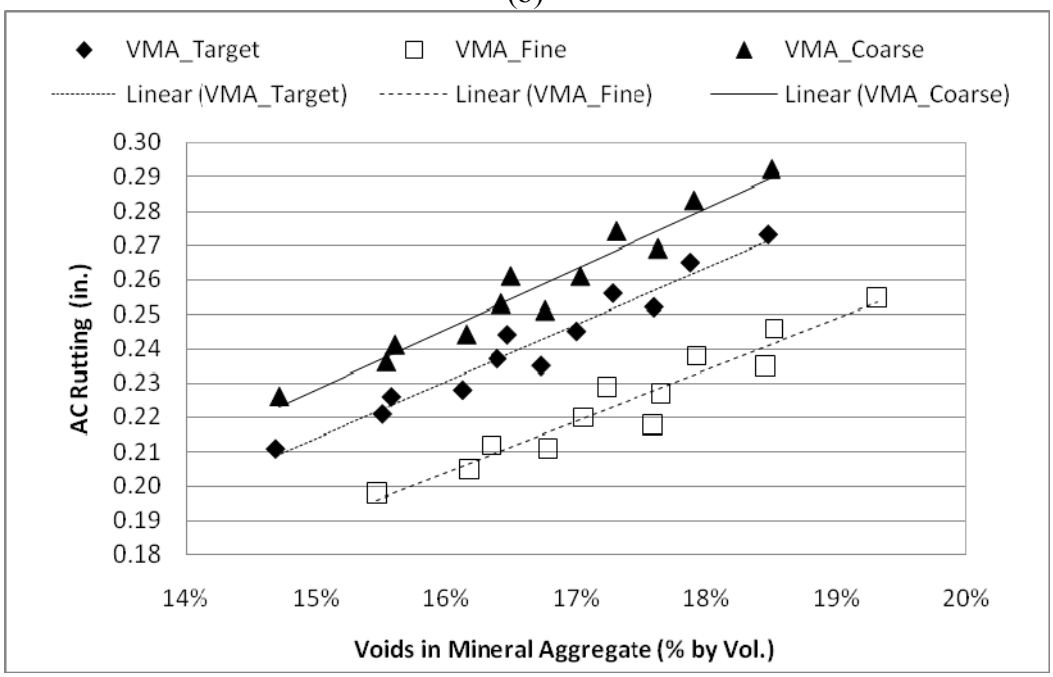

(c)

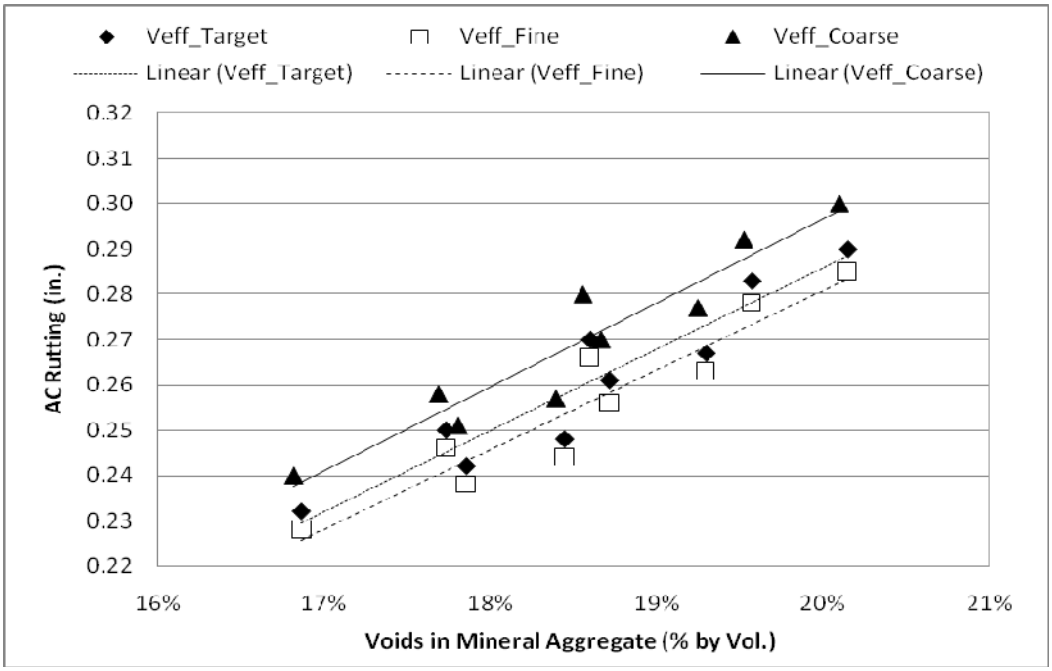

Figure 4.2 Voids in mineral aggregate vs. AC rutting for Types *(a)* C, *(b)* D, and *(c)* SMA D

4.1.3. Overall Mixture Performance Based on VMA

When comparing the mixtures against each other, several significant trends were observed. For example, it was observed that overall the pavement sections modeled with the Type C mixture had the best performance out of the three mixtures, the overall lowest percentage of VMA by volume and the lowest variability. The pavement sections modeled with the Type D mixture showed the highest asphalt rutting and the highest variability, while the SMA-D mixture was somewhere in between.

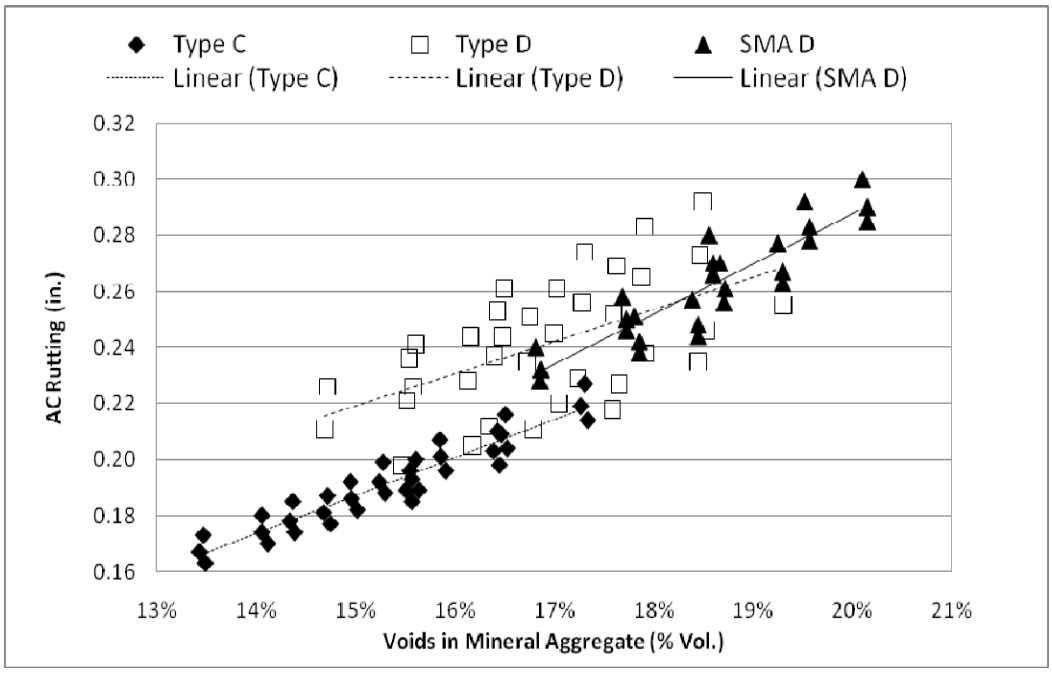

Figure 4.3 MEPDG results for VMA vs. AC rutting

By using simple regression analysis and developing trend lines for each mixture type and observing their slopes, it was observed that VMA had the least significant effect on asphalt rutting for the Type D mixture and the most significant effect for the SMA-D mixture. These trends are shown in Figure 4.3 above and the statistics from the regression analysis can be viewed in Table 4.1.

From the statistical analysis a strong linear relationship was also observed between the voids in mineral aggregate and pavement rutting for all three mixes. By observing the coefficient of determination (R^2) it can be inferred that these simple regression models do an adequate job at explaining the variability in the data for Type C and SMA-D mixtures. Although there is a significant amount of unexplained variability in the data for the Type D model, by observing Figure 4.3, it can be seen that there is still a strong linear relationship between voids in mineral aggregate and rutting in the AC layer.

Table 4.1 Regression Statistics for the Three Mixes (Type C, Type D, and SMA-D)

Statistics	Type C	Type D	SMA-D
Intercept	-0.016	0.046	-0.069
Slope	1.355	1.155	1.785
P-Value	1.38E-17	2.86E-04	2.33E-10
R^2	88.6%	32.5%	80.5%

4.1.4. Overall Mixture Performance Based on VFA

The performance of mixtures can also be compared against each other by observing the voids filled with asphalt (VFA). In Figure 4.4, the results of the pavement sections modeled with a 93% relative density are shown. It can be observed that for all three mixtures, asphalt rutting increased with higher percentages of VFA. It can also be observed that, in general, VFA is a good indicator of rutting. Mixtures with higher VFAs tended to experience more rutting. For example, the Type C mixture had the overall lowest percentage of VFA, and as shown in Figure 4.4, it also had the overall best performance out of the three mixes. Type D and SMA-D mixes performed very similarly as predicted by the MEPDG, however, the SMA-D showed less variability.

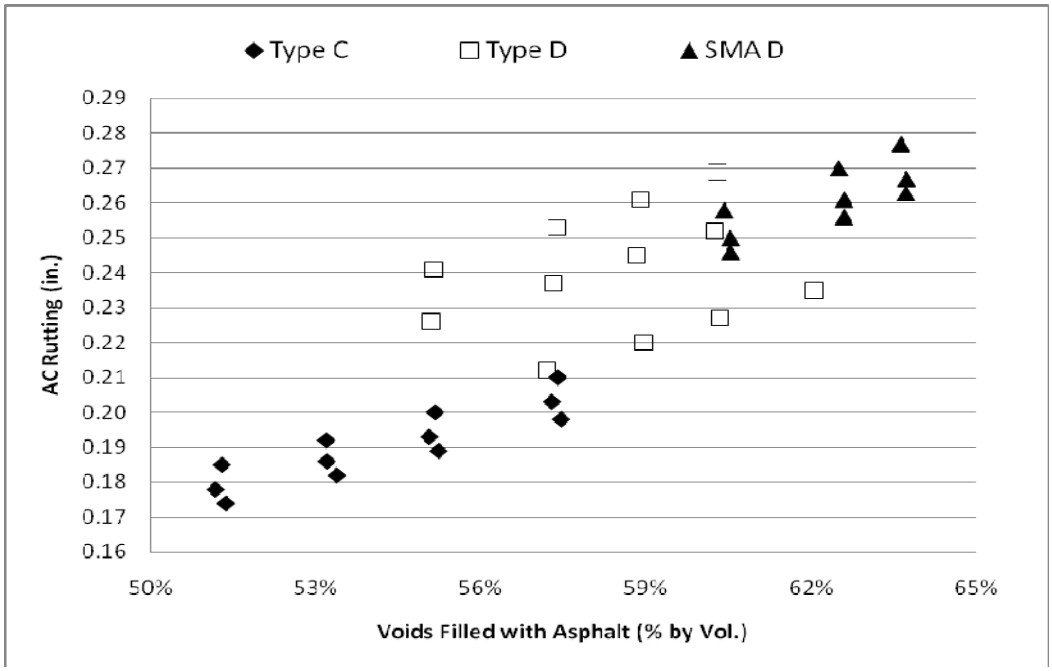

Figure 4.4 MEPDG results for VFA vs. AC rutting at 93% density

4.2. HWTD RESULTS

This section compares the results from the MEPDG analysis to the results from the HWTD test. In order to do so effectively, only those specimens that were modeled at a density of 93% (7% air voids) were chosen to be compared to the results from the HWTD. Since the results of the sensitivity analysis were presented and discussed in the previous section, the reader could easily discern how specimens modeled at a 92% density or a 94% density would compare to the HWTD results.

4.2.1. Coarser Dense-Graded Hot-Mix Asphalt Mixture: TxDOT Type C

Figures 4.5 to 4.7 show the life-cycle performance for the Type C limestone mixture under, (a) the MEPDG, and (b) the Hamburg Wheel Tracking Device. From the figures it can be seen that the MEPDG predicted similar trends to those measured in the laboratory by the HWTD. The most significant difference between the MEPDG and the HWTD is that the MEPDG predicts lower sensitivity of the mixes to asphalt content. In this particular case, the laboratory results seem more reasonable.

(a)

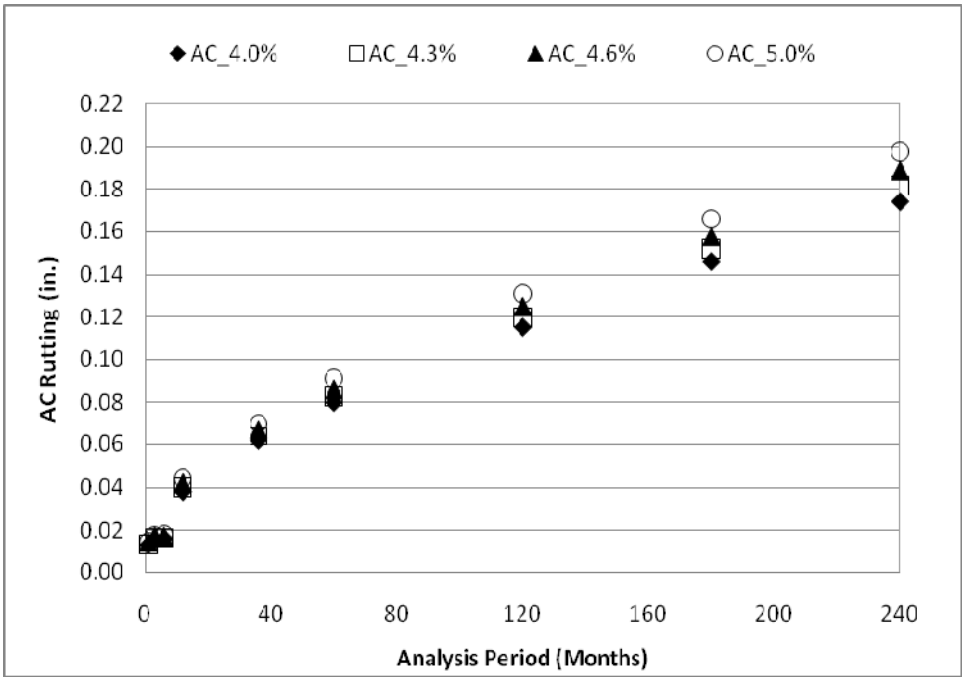

(b)

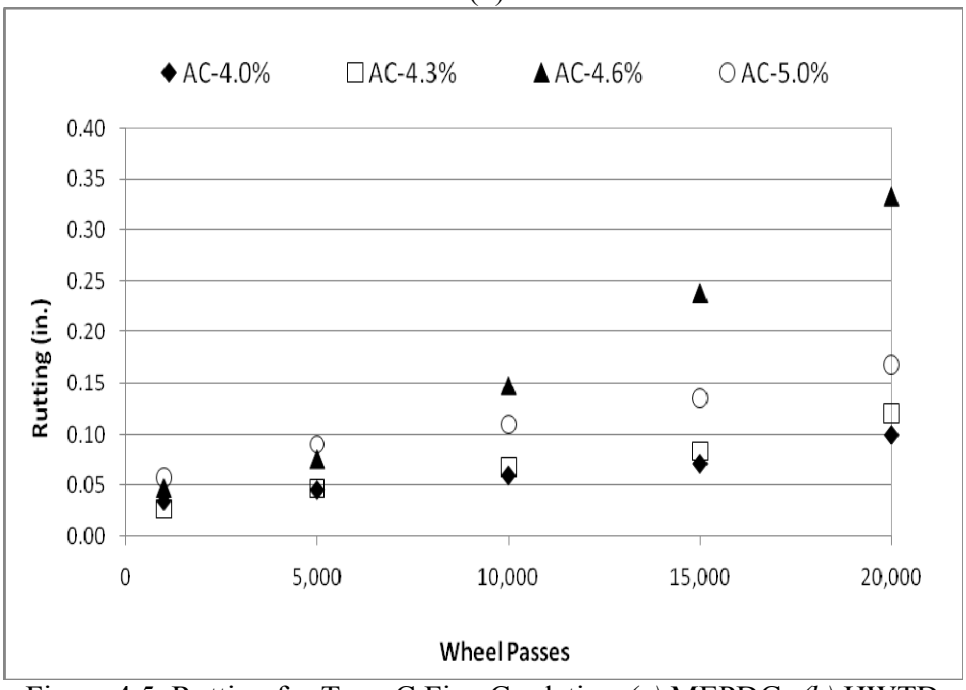

Figure 4.5 Rutting for Type C Fine Gradation *(a)* MEPDG, *(b)* HWTD

(a)

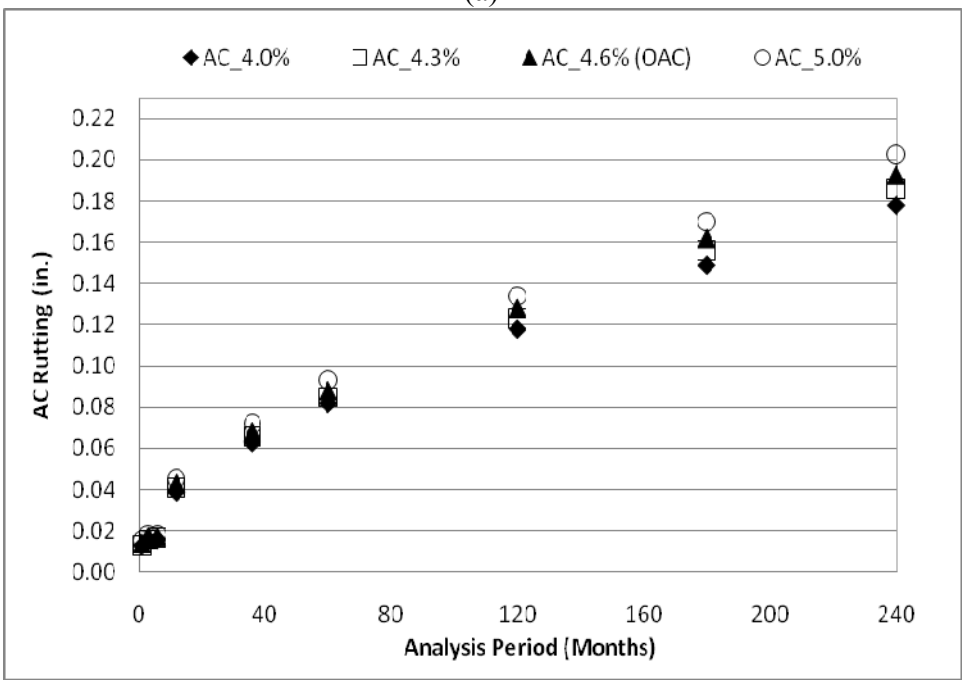

(b)

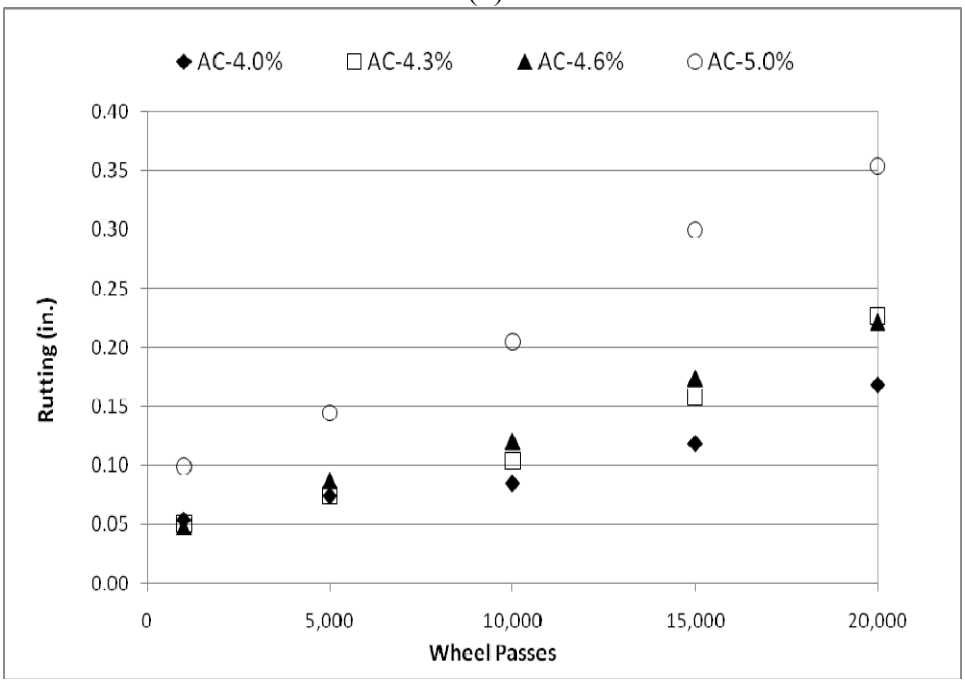

Figure 4.6 Rutting for Type C Target Gradation *(a)* MEPDG, *(b)* HWTD

(a)

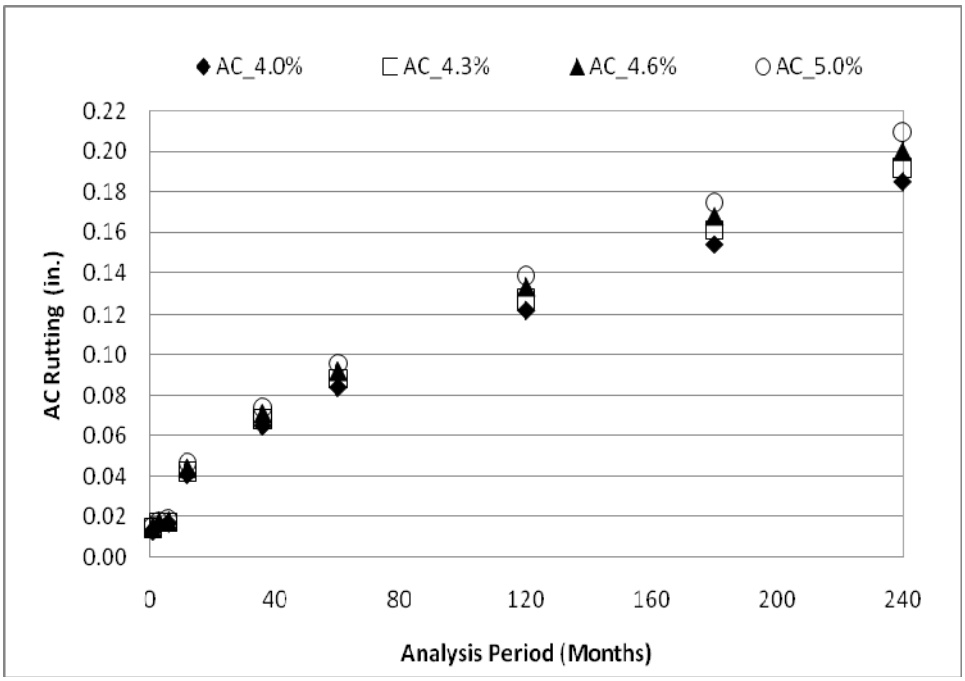

(b)

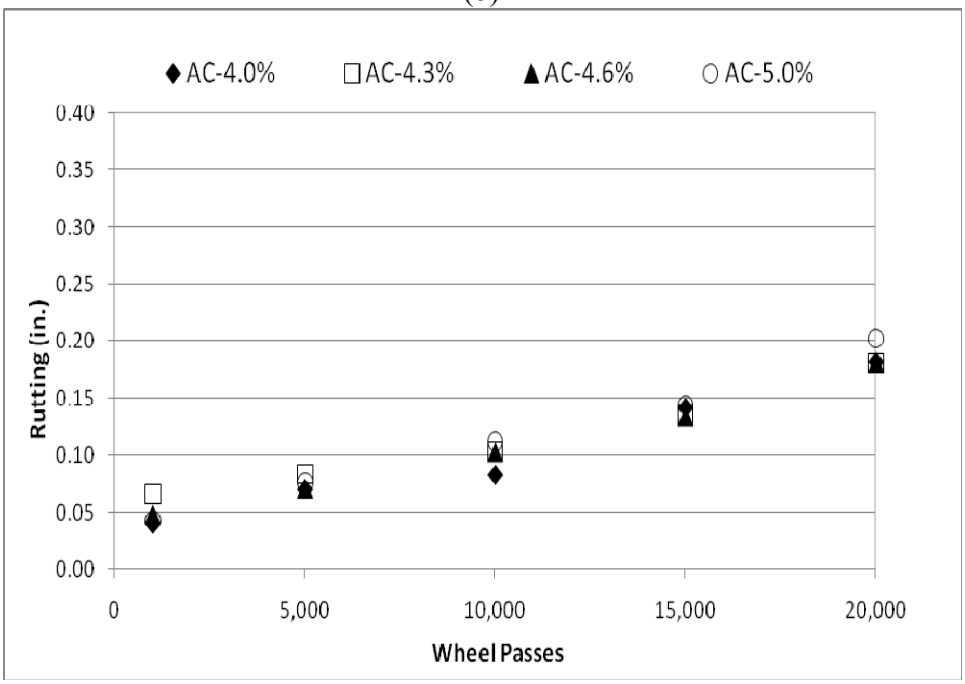

Figure 4.7 Rutting for Type C Coarse Gradation *(a)* MEPDG, *(b)* HWTD

Table 4.2 ranks in order (1 being the best and 4 the worst) the performance of specimens by their gradation and binder content. It can be seen that both MEPDG and the HWTD produced similar results.

Table 4.2 Ranking of Results for TxDOT Type C

	Fine Gradation		Target Gradation		Coarse Gradation	
	MEPDG	HWTD	MEPDG	HWTD	MEPDG	HWTD
1	4.0%	4.0%	4.0%	4.0%	4.0%	4.3%
2	4.3%	4.3%	4.3%	4.6%	4.3%	4.0%
3	4.6%	5.0%	4.6%	4.3%	4.6%	4.6%
4	5.0%	4.6%	5.0%	5.0%	5.0%	5.0%

To further analyze the data, the effects of binder content on the rutting of the asphalt mixture (Type C) as predicted by the MEPDG and as measured under the HWTD were plotted in Figure 4.8. From Figure 4.8 it can be seen that for both the MEPDG and the HWTD rutting increases with higher amounts of binder content by weight. It can also be seen that for all binder contents, the MEPDG predicts sections with a finer gradation to perform the best, and sections with a coarser gradation to perform the worst. This was not always the case with the results seen from the HWTD.

(a)

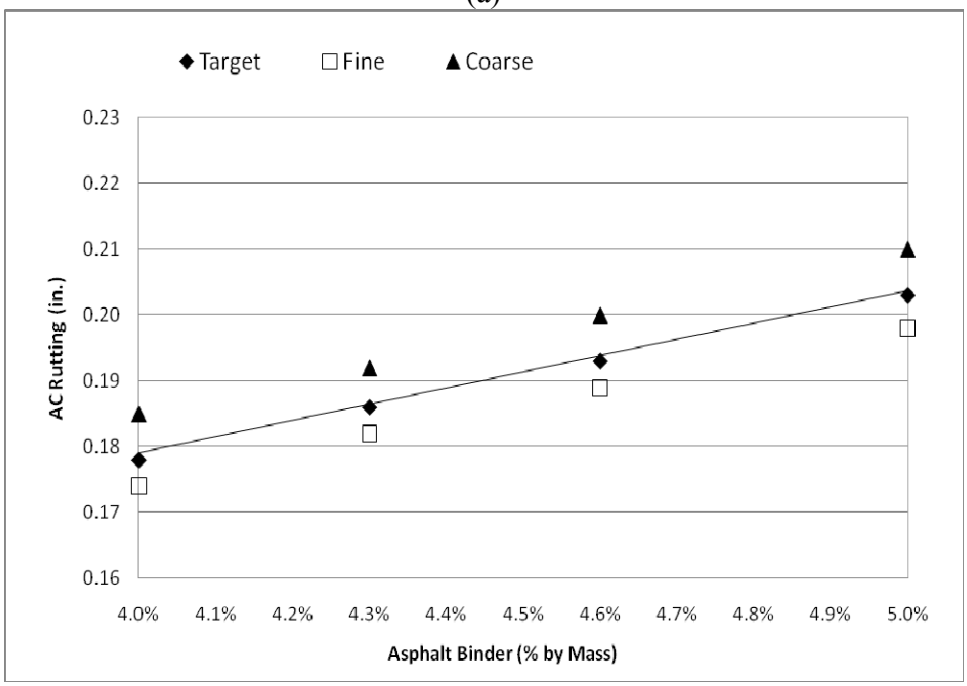

(b)

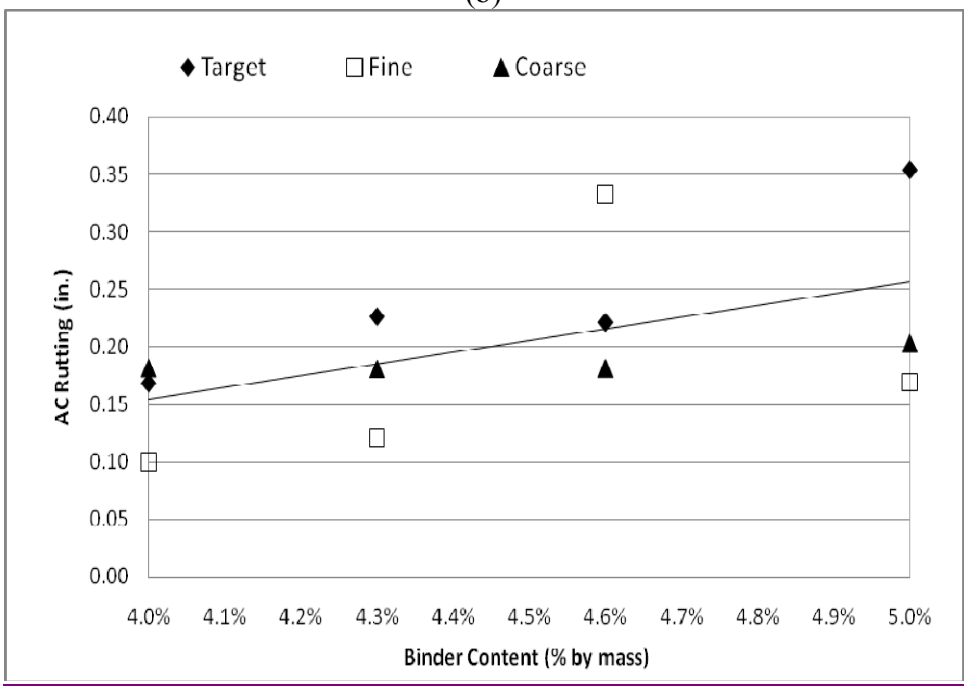

Figure 4.8 Binder Content by Mass vs. Rutting for Type C *(a)* MEPDG, *(b)* HWTD

To quantify these effects, a simple regression was conducted, and the statistics are in Table 4.3. From the asphalt content coefficient and its p-value, it can be seen that there is a strong linear relationship between binder content and rutting for both the MEPDG and HWTD. Looking at the effects of gradation, for the MEPDG results it can be seen that mixes on the finer side of the allowable tolerances experienced less rutting (negative sign) than mixes with a target gradation (as per JMF), while mixes that were on the coarser side of the allowable tolerances experienced more rutting (positive sign). These differences were statistically significant. For the HWTD, mixes that were either on the coarser or finer side of the target gradation, on average experienced less rutting however, these differences were not found to be statistically significant. It should be also noted that the variability of the HWTD results is significantly higher, as expected.

Table 4.3 Regression Statistics for TxDOT Type C

Statistics	MEPDG		HWTD	
	Coefficient	P-Value	Coefficient	P-Value
AC	2.463	8.75E-13	10.193	0.085
Fine	-0.004	4.46E-07	-0.062	0.224
Coarse	0.007	1.19E-08	-0.056	0.268
R^2	99.9%		42.7%	

To undestand the effects of the selected gradation on pavement rutting, the performance of the three levels of gradation within the Type C master gradation band were plotted against binder content. From the MEPDG results (Figure 4.9a), it can be seen that there is positive correlation: rutting in the asphalt layer tends to increase as the gradation moves from the finer side to the coarser side of the gradation band. The trends observed from the HWTD results (Figure 4.9b) are a bit different. On avergae, rutting tends to increase as the level of gradation moves from fine to corase, however, this trend is not statistically significant. For asphalt content of 4.6%, which was determined to be the OAC, rutting measured by the HWTD significantly decreases as the level of gradation moves from fine to coarse.

(a)

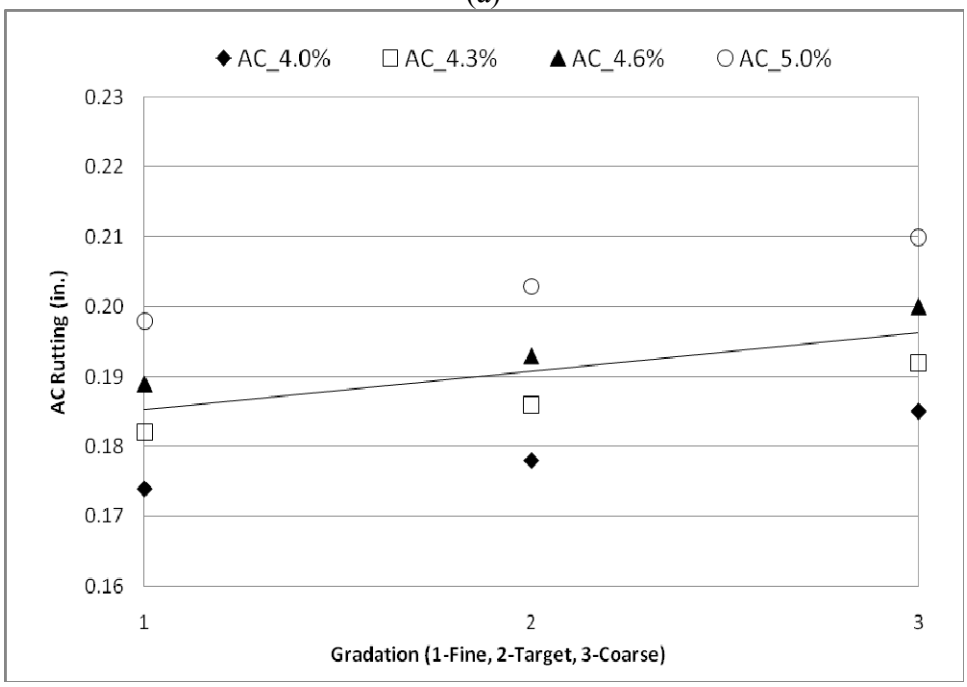

(b)

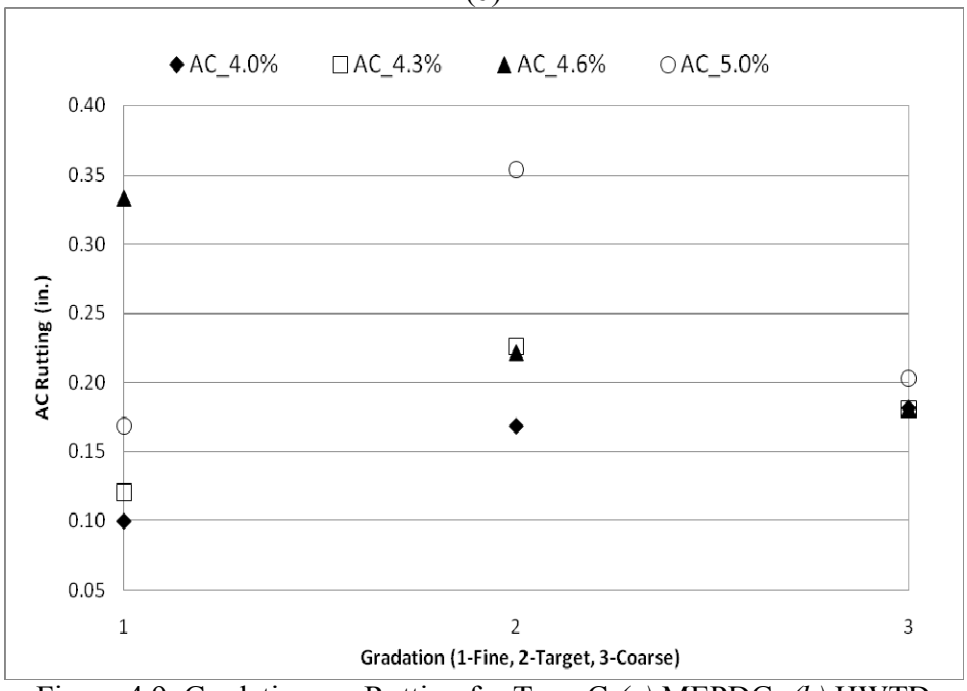

Figure 4.9 Gradation vs. Rutting for Type C *(a)* MEPDG, *(b)* HWTD

4.2.2. Finer Dense-Graded Hot-Mix Asphalt Mixture: TxDOT Type D

Figures 4.10 through 4.12 show the life-cycle performance for Type D limestone mixture under, (a) the MEPDG, and (b) the Hamburg Wheel Tracking Device. From the figures it can be seen that the MEPDG predicted similar results to those measured by the HWTD.

(a)

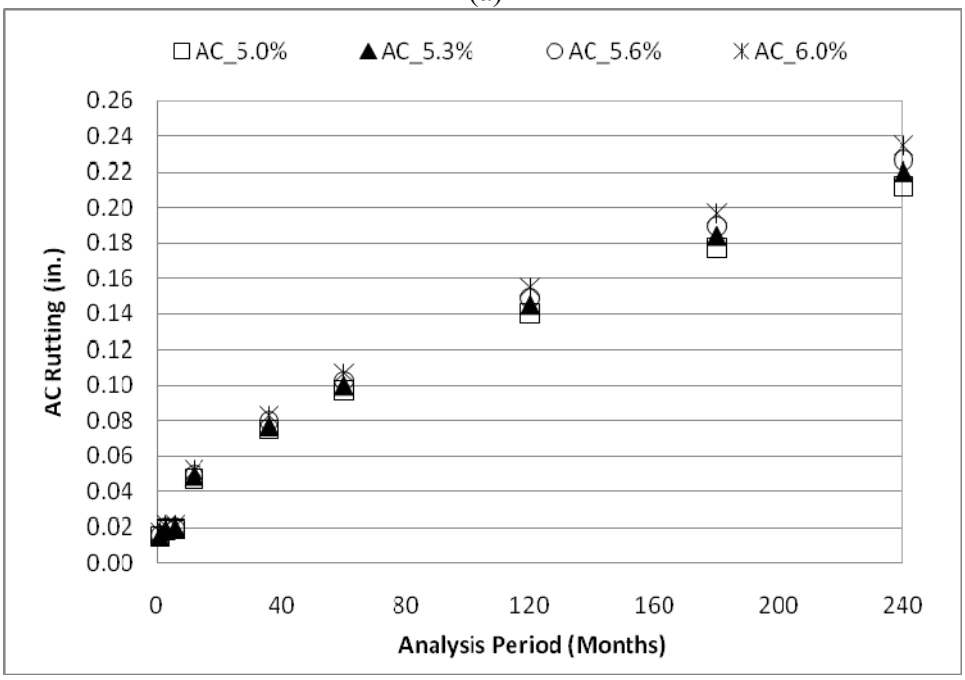

(b)

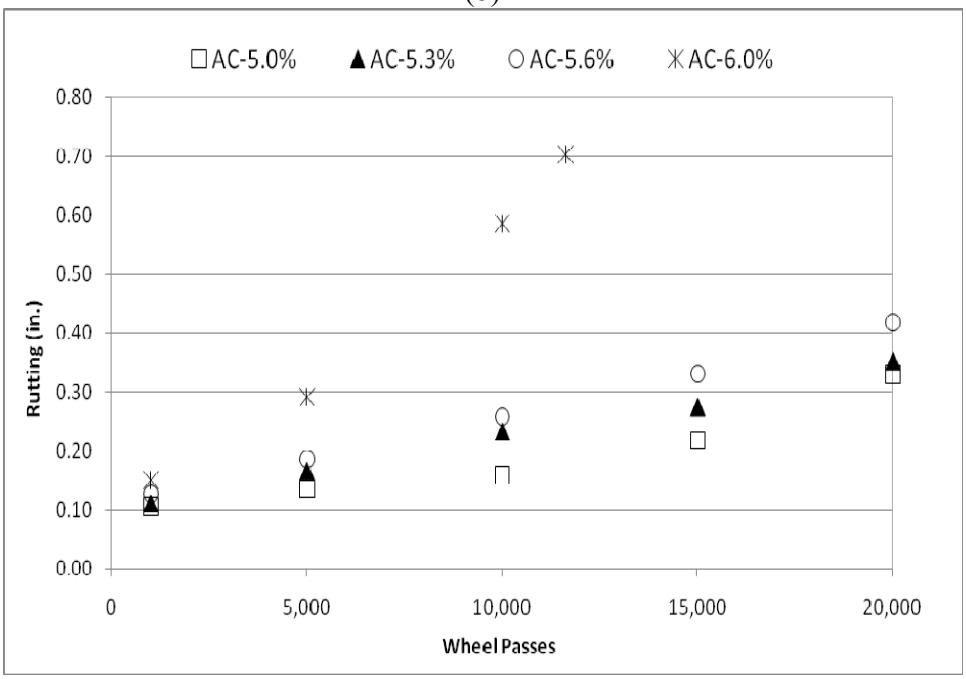

Figure 4. 10 Rutting for Type D Fine Gradation *(a)* MEPDG, *(b)* HWTD

(a)

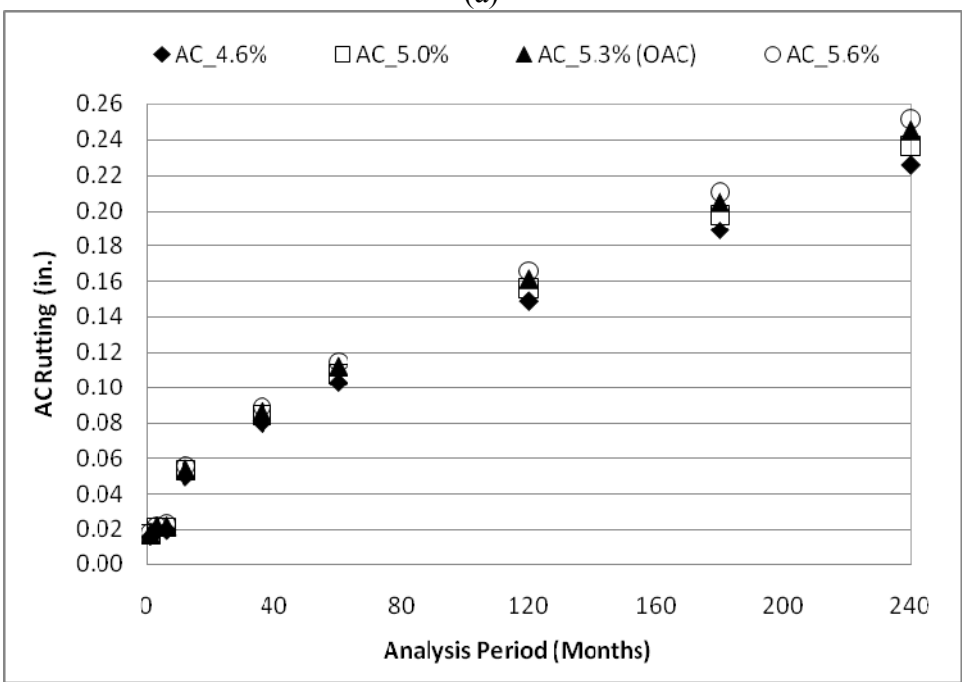

(b)

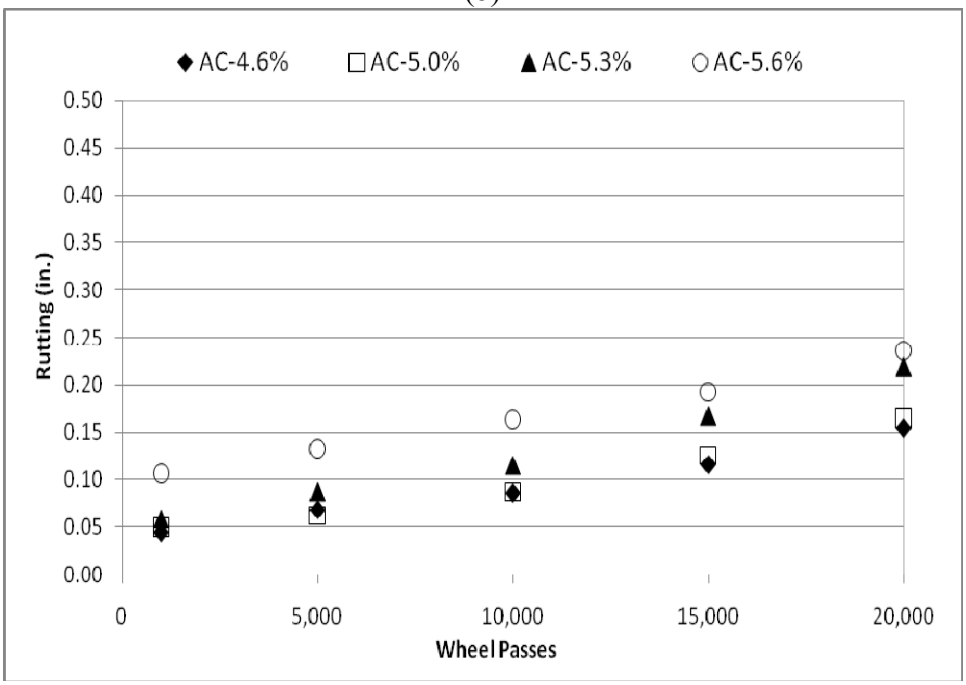

Figure 4.11 Rutting for Type D Target Gradation *(a)* MEPDG, *(b)* HWTD

(a)

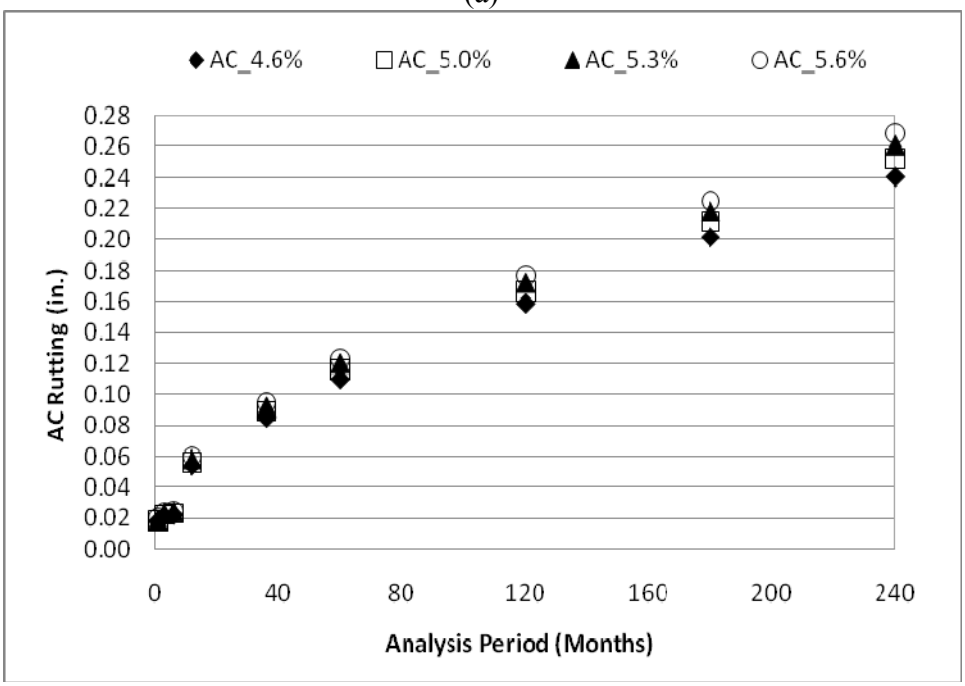

(b)

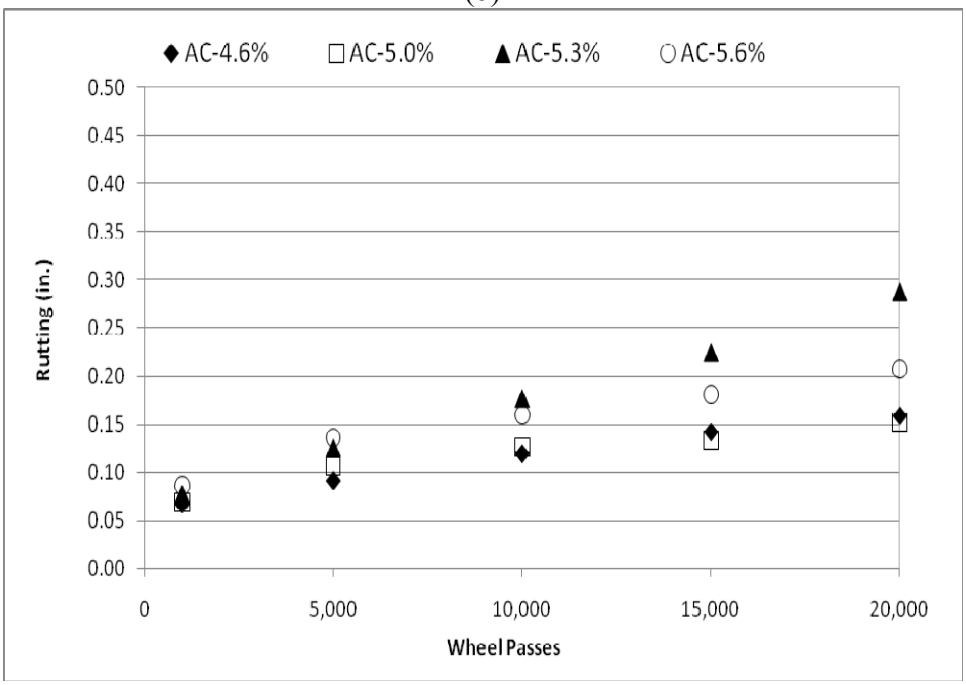

Figure 4.12 Rutting for Type D Coarse Gradation *(a)* MEPDG, *(b)* HWTD

Table 4.4 ranks in order (1 being the best and 4 the worst) the performance of specimens by their gradation and binder content. It can be seen that both MEPDG and HWTD produced similar results.

Table 4.4 Rankings of Results for TxDOT Type D

	Fine Gradation		Target Gradation		Coarse Gradation	
	MEPDG	HWTD	MEPDG	HWTD	MEPDG	HWTD
1	5.0%	5.0%	4.6%	4.6%	4.6%	5.0%
2	5.3%	5.3%	5.0%	5.0%	5.0%	4.6%
3	5.6%	5.6%	5.3%	5.3%	5.3%	5.6%
4	6.0%	6.0%	5.6%	5.6%	5.6%	5.3%

To show the effects of binder content, asphalt rutting predicted by the MEPDG and measured under the HWTD were plotted in Figure 4.13a and 4.13b. It can be seen that for both the MEPDG and the HWTD rutting increases with higher amounts of binder content by weight. Although both the tests predicted an overall positive trend, it should be noted that there is significant disparity among the data. For example, in the MEPDG analysis specimens with a finer level of gradation tended to perform the best while in the HWTD analysis specimens with a finer level of gradation tended to perform the worst. Therefore, even though the model embedded in the MEPDG has good predictive capabilities, these capabilities could be further improved by incorporating data from performance-related testing and, ultimately, from field sections.

(a)

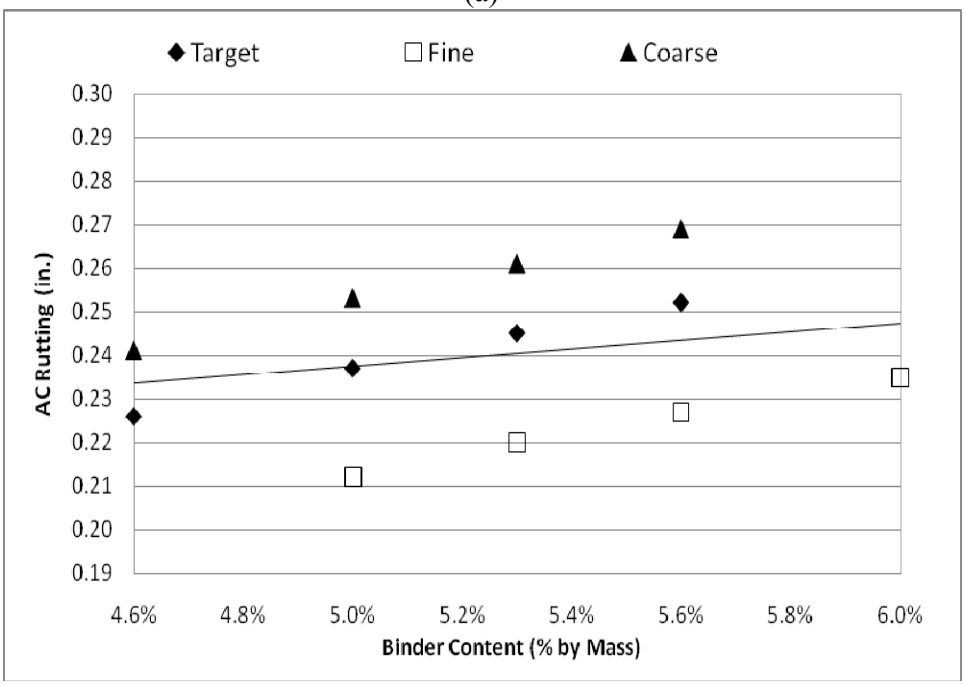

(b)

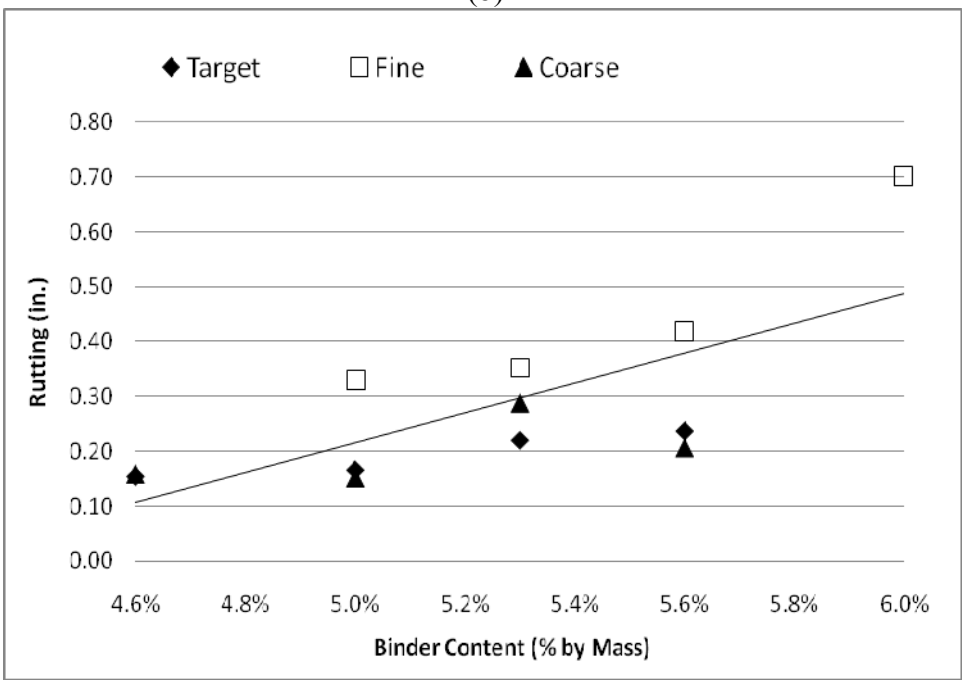

Figure 4.13 Binder Content vs. Rutting for Type D *(a)* MEPDG, *(b)* HWTD

To further examine these findings, a simple regression was conducted and the results are shown in Table 4.5. By observing the AC coefficient and its p-value, again it can be seen that a strong linear relationship exists between binder content and rutting for both the MEPDG and

HWTD. Looking at the effects of gradation, for the MEPDG it can be seen that finer mixes rut less than mixes with a target gradation, while coarser mixes rut more. For the MEPDG this variability in gradation was found to be significant. For the HWTD, both coarser and finer mixes experienced more rutting than target mixes, however only the variability of the finer mixes was found to be statistically significant.

Table 4.5 Regression Statistics for TxDOT Type D

Statistics	MEPDG		HWTD	
	Coefficient	P-Value	Coefficient	P-Value
AC	2.566	1.48E-09	18.140	0.020
Fine	-0.025	1.24E-09	0.194	0.013
Coarse	0.016	2.84E-08	0.008	0.889
R^2	99.7%		81.5%	

To further undestand these effects, the three levels of gradation within the Type D master gradation band were plotted against rutting. From the MEPDG results (Figure 4.14a), it can be seen that there is a positive correlation: rutting in the asphalt layer increases as the level of gradation moves from the finer to coarser side of the gradation band. The equivalent trends observed from the HWTD results (Figure 4.14b) show that rutting was measured at its lowest at the target level and increases when moving to either the finer or coarser side of the tolerences. However, the difference in rutting between target and coarse gradations was not significant. Also variability amongst the performance results was at its lowest at target gradation.

(a)

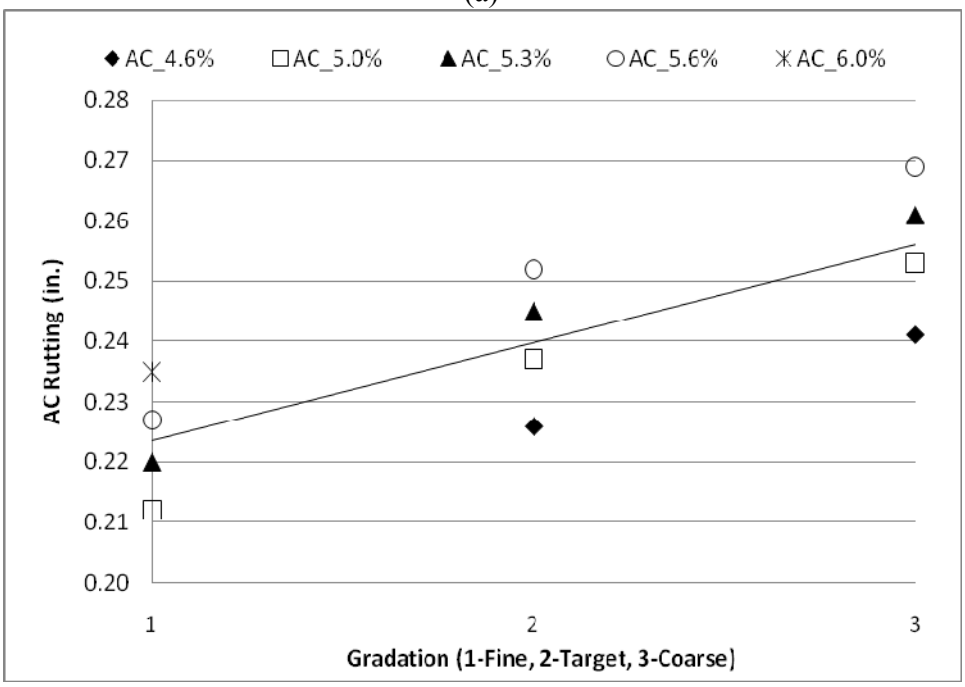

(b)

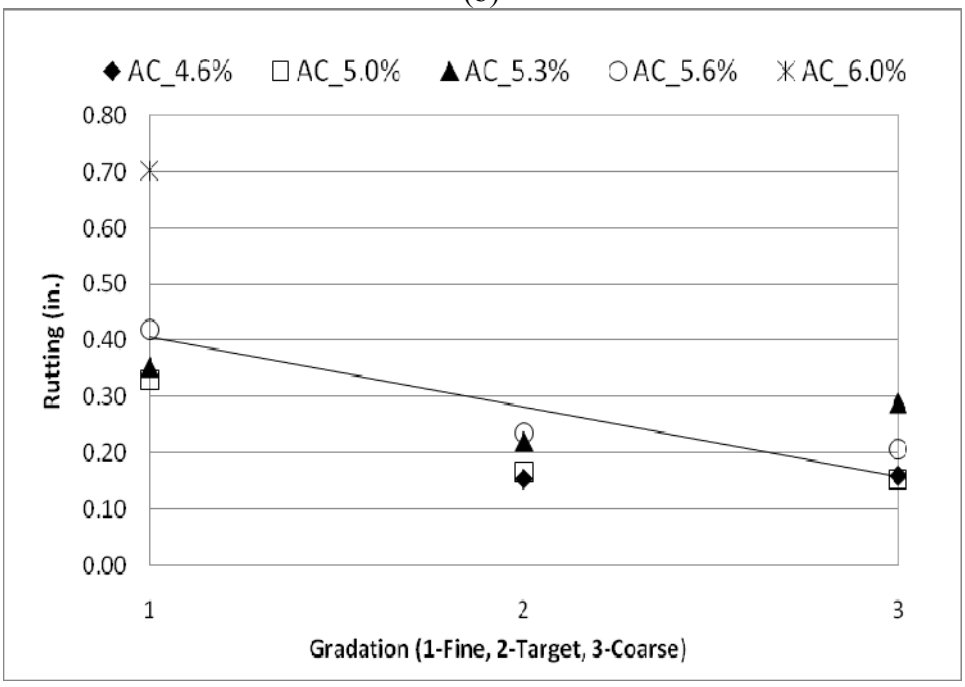

Figure 4.14 Gradation vs. Rutting for Type D *(a)* MEPDG, *(b)* HWTD

4.2.3. Stone Matrix Asphalt Mixture: TxDOT SMA-D

Figures 4.15 through 4.17 show the life-cycle performance for the SMA-D limestone mixture under, (a) the MEPDG, and (b) the Hamburg Wheel Tracking Device. From the figures it can bee seen that both MEPDG and the HWTD predicted similar results.

(a)

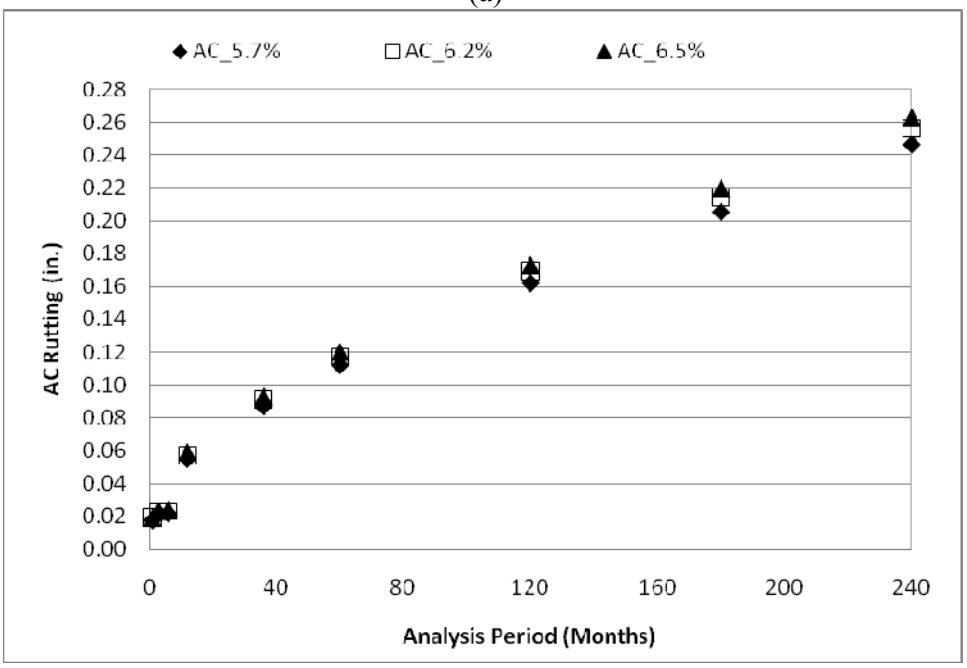

(b)

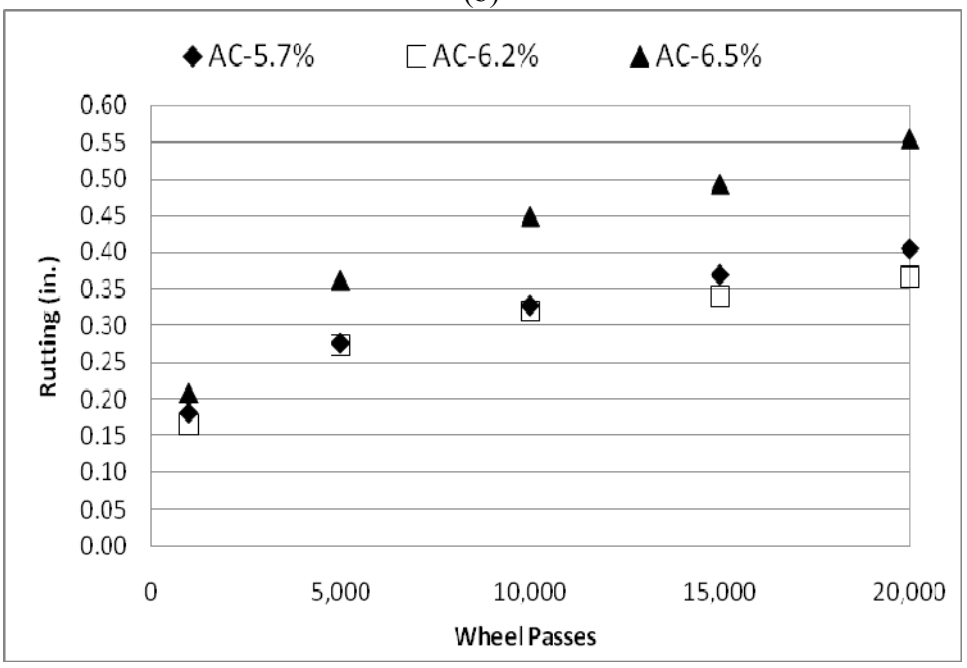

Figure 4.15 Rutting for SMA D Fine Gradation *(a)* MEPDG, *(b)* HWTD
(a)

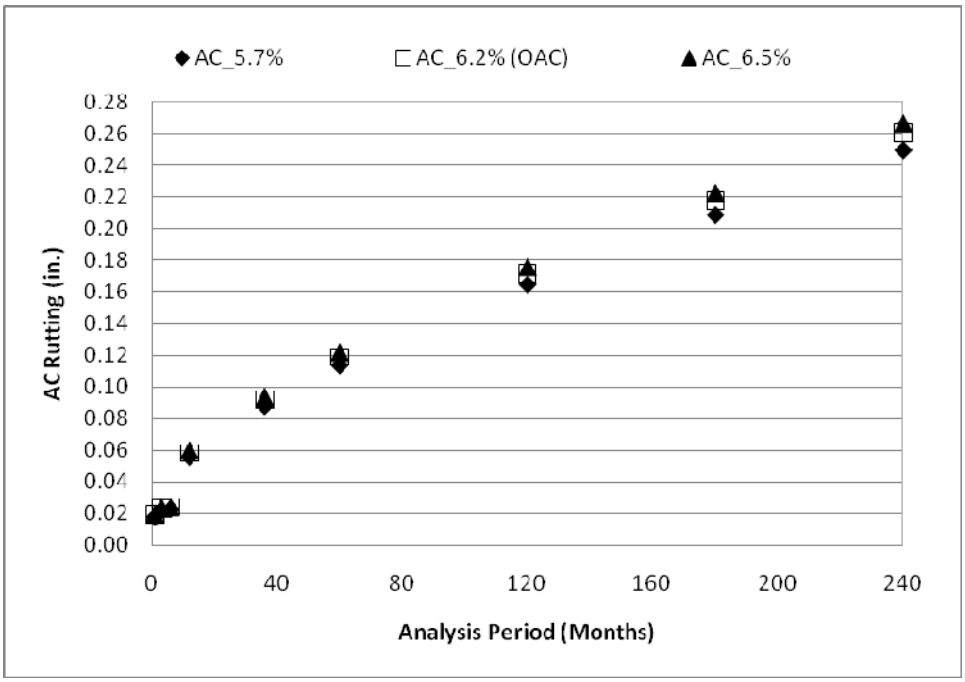

(b)

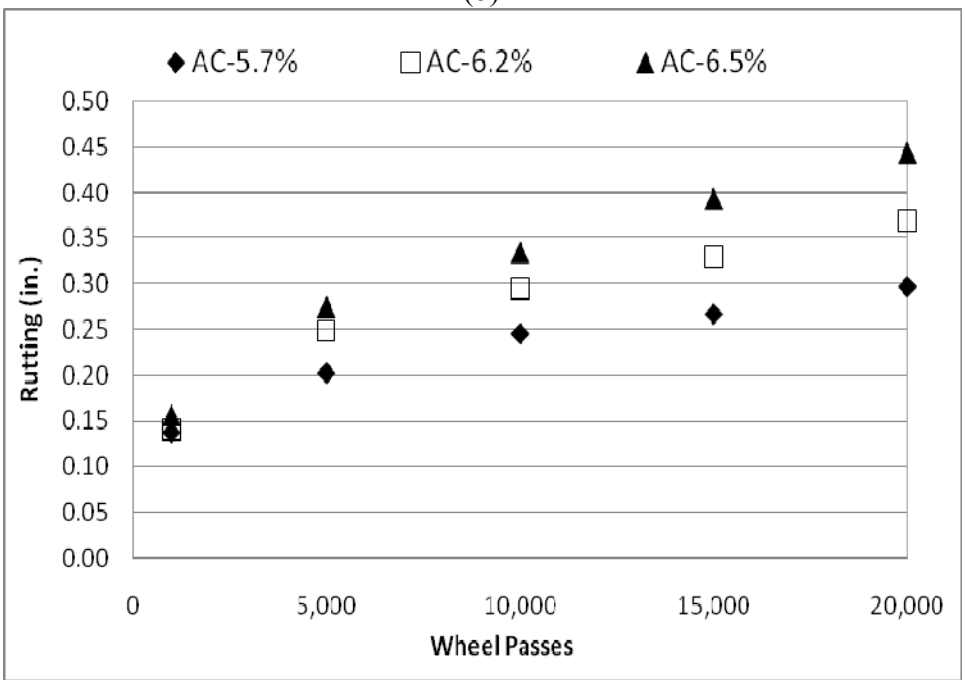

Figure 4.16 Rutting for SMA D Target Gradation *(a)* MEPDG, *(b)* HWTD

(a)

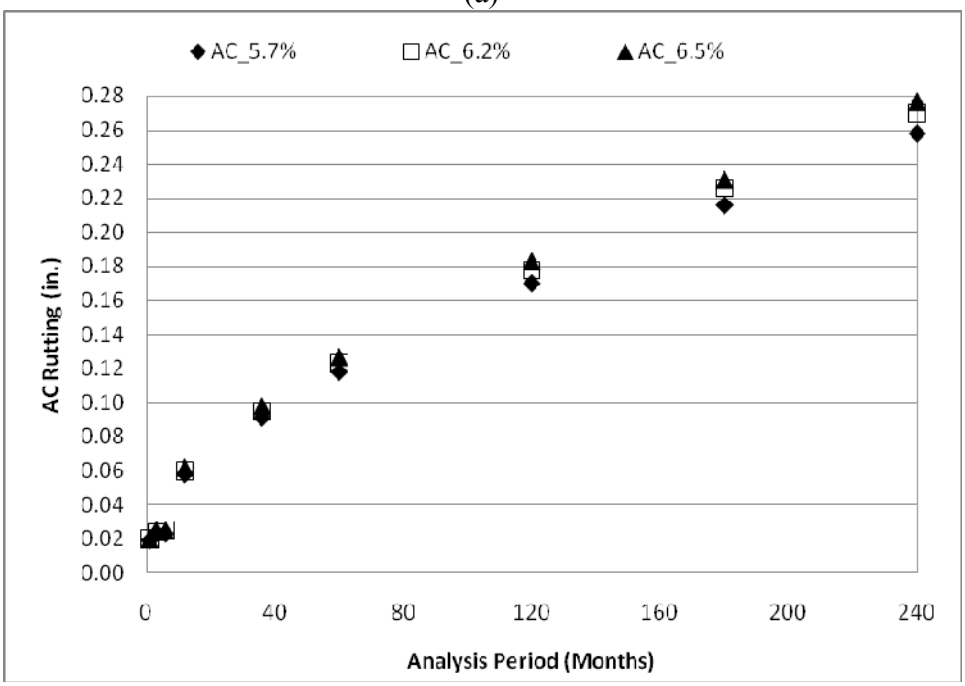

(b)

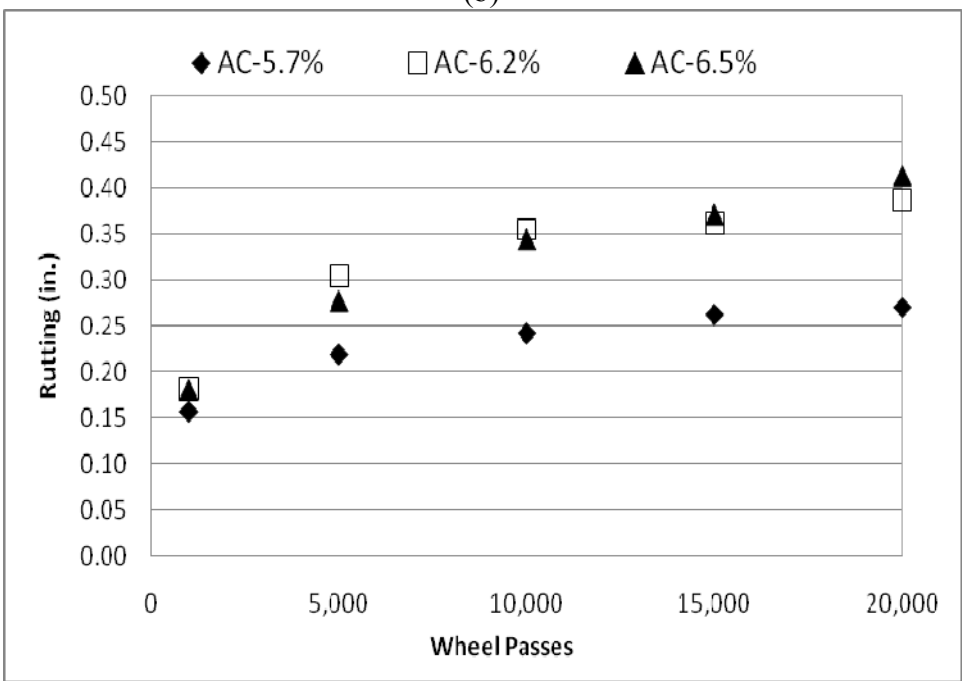

Figure 4.17 Rutting for SMA D Coarse Gradation *(a)* MEPDG, *(b)* HWTD

Table 4.6 ranks in order (1 being the best and 3 the worst) the performance of specimens by their gradation and binder content.

Table 4.6 Ranking of Results for TxDOT SMA D

	Fine Gradation		Target Gradation		Coarse Gradation	
	MEPDG	HWTD	MEPDG	HWTD	MEPDG	HWTD
1	5.7%	6.2%	5.7%	5.7%	5.7%	5.7%
2	6.2%	5.7%	6.2%	6.2%	6.2%	6.2%
3	6.5%	6.5%	6.5%	6.5%	6.5%	6.5%

To compare the effects of binder content on asphalt rutting predicted by the MEPDG and measured under the HWTD, the results were plotted in Figure 4.18a and 4.18b. It can be seen that for both the MEPDG and the HWTD rutting increases with higher binder content by weight; nevertheless, it should be noted that, once again, there is some disparity among the data. It can be seen that the MEPDG analysis predicted mixes with a finer level of gradation to perform the best while the HWTD analysis measured specimens with a finer level of gradation to perform the worst.

(a)

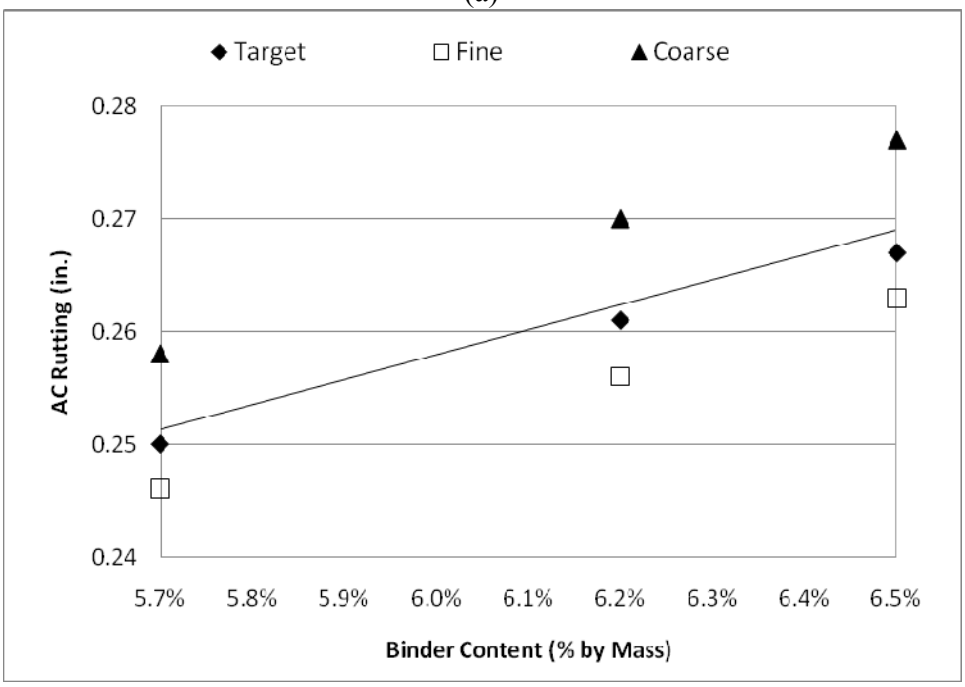

(b)

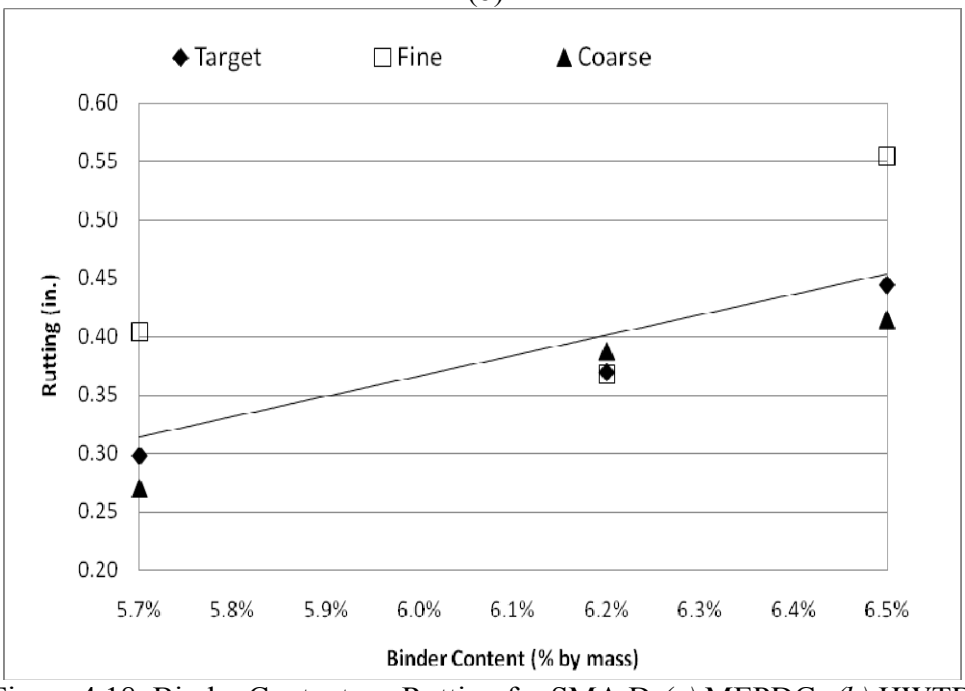

Figure 4.18 Binder Content vs. Rutting for SMA D *(a)* MEPDG, *(b)* HWTD

To further examine these findings a simple regression was conducted and the regression statistics are shown in Table 4.7. From the AC parameter and the p-value it can be seen that a strong linear relationship exists between binder content by mass and rutting for both models. Looking at the effects of gradation, for MEPDG it can be seen that finer mixes tended to experience less rutting while coarser mixes tended to experience more rutting and both of these

trends were statistically significant. From the HWTD analysis, the opposite trends can be seen, but these trends are not statistically significant.

Table 4.7 Regression Statistics for TxDOT SMA-D

Statistics	MEPDG		HWTD	
	Coefficient	P-Value	Coefficient	P-Value
AC	2.207	2.86E-07	17.503	0.017
Fine	-0.004	2.99E-07	0.072	0.132
Coarse	0.009	8.56E-06	-0.013	0.761
R^2	99.8%		78.1%	

When the the rutting is displayed for the three levels of gradation, the disparity in the data can be fully analyzed. From the MEPDG results (Figure 4.19a), it can be seen that there is a positive correlation: rutting in the AC layer increases as the level of gradation moves from the finer side to the coarser side of the gradation band. The trends observed from the HWTD results (Figure 4.19b) seem to be completely opposite, with rutting in the specimen actually decreasing as the level of gradation moves from the finer side to the coarser side of the gradation band. Most likely, the HWTD testing is too variable to capture the relative small difference in these gradations.

(a)

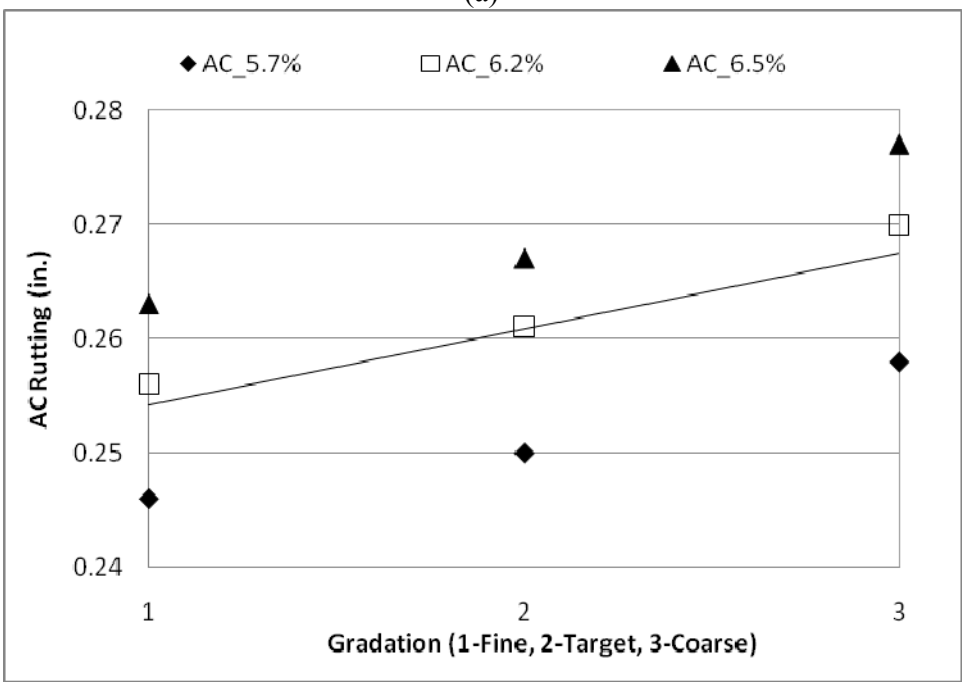

(b)

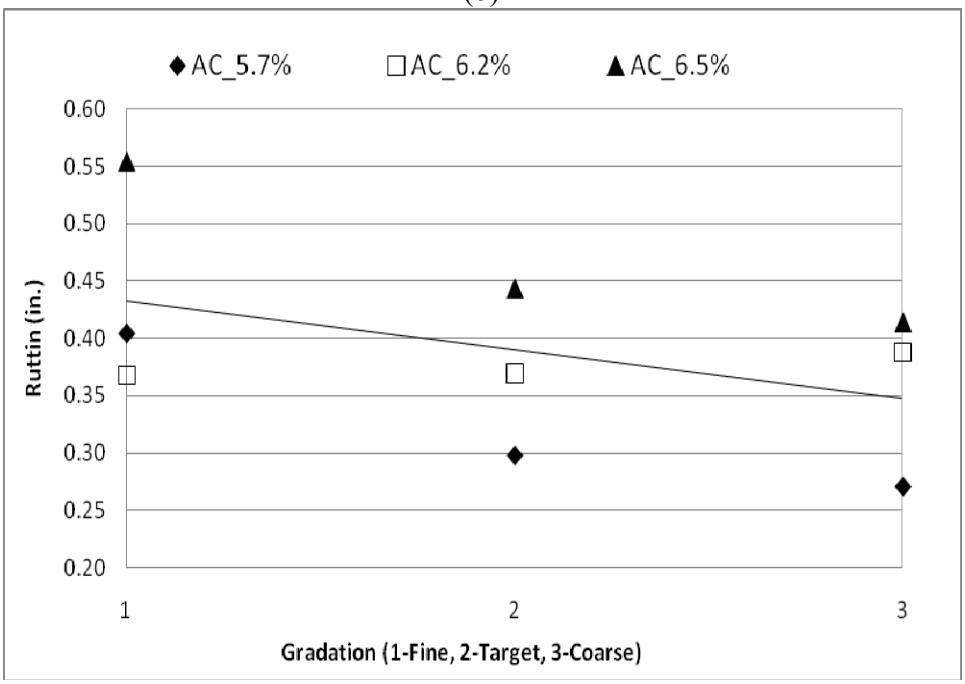

Figure 4.19 Gradation vs. Rutting for Type D *(a)* MEPDG, *(b)* HWTD

CHAPTER 5-CONCLUSIONS

The main conclusion of this study indicates that the asphalt rutting performance predictions obtained from the MEPDG analysis support the laboratory results obtained from the Hamburg Wheel Tracking Device test. From Figure 5.1, it can be seen that both the MEPDG and the HWTD ranked the coarser dense-graded hot-mix asphalt mixture (TxDOT Type C) to perform the best, followed by the finer dense-graded hot-mix asphalt mixture (TxDOT Type D) and lastly the stone matrix asphalt mixture (TxDOT SMA-D).

(a)

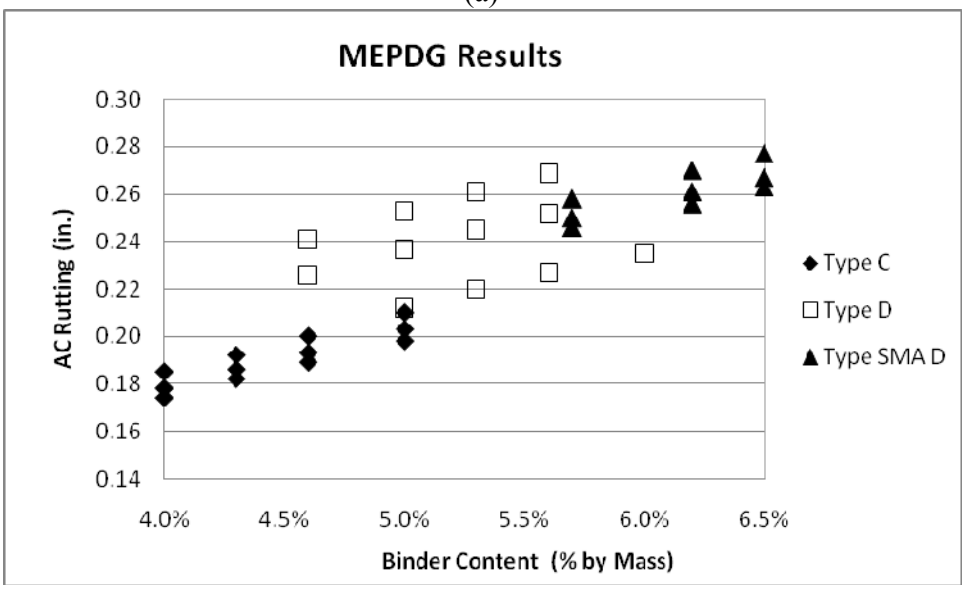

(b)

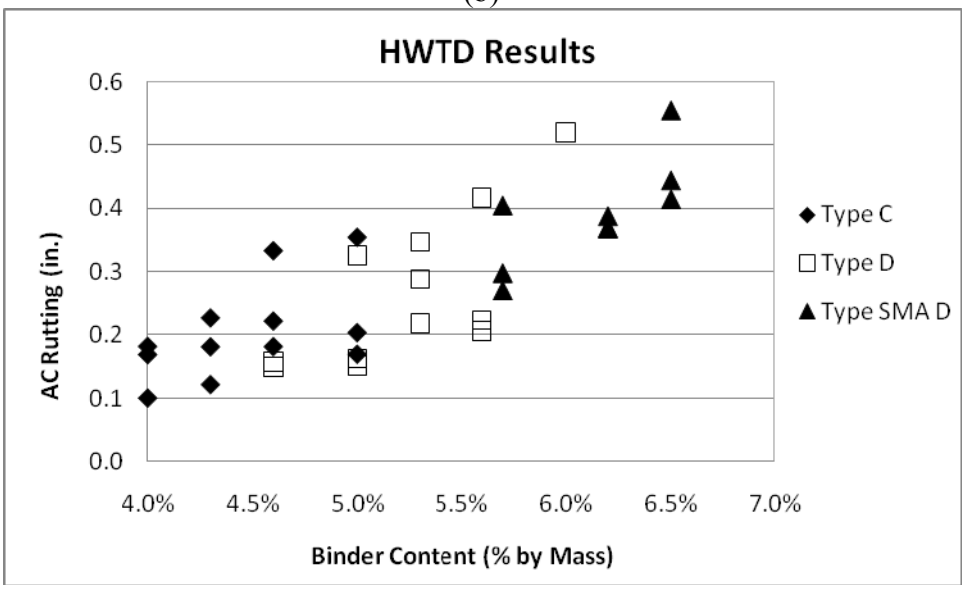

Figure 5.1 Overall Performance *(a)* MEPDG, *(b)* HWTD

Mechanistic-empirical predictions and laboratory results also showed that for all three mixtures pavement rutting increased with higher amounts of binder content by weight. Furthermore, this study allowed the rutting sensitivity of the various mixes to be quantified as a function of their binder content.

It was also concluded that although the overall results from the MEPDG support the results from the HWTD, the MEPDG could not effectively predict the effects of slight variability within each mixture's allowable tolerance on pavement performance. For all three mixtures, the MEPDG predicts less rutting in the asphalt layer for those specimens whose gradation shift to the finer side of the target gradation determined by the job mix formula and more rutting for those mixes whose gradation shift to the coarser side of the allowable tolerances.

From the analysis of the HWTD results, it was observed that the two finer mixtures, Type D and SMA-D, actually showed opposite results. For the Type D mixture, the HWTD results showed that specimens with a target gradation performed the best followed by specimens with a coarser gradation, while specimens with a finer gradation performed significantly worst than the previous two, showing 123% more rutting. For the SMA-D mixture, it was observed that specimens on the coarser side of the tolerance, performed better than specimens on the finer side but, on average, the difference in performance was rather small (only 19%) as compared to the difference with the Type D mixture.

The lack of sensitivity in the prediction of the effects of slight variability in gradation on pavement performance may point out to the need for an updated and revised version of Witczak's dynamic modulus predictive equation. Since the equation only uses four sieve sizes to capture the entire aggregate gradation, it may not be highly sensitive to minor changes as those typical of allowable tolerances. If the predicted dynamic modulus is not sensitive to small changes in gradation, the mechanical responses which are computed by JULEA and used in the distress prediction models will also lack sensitivity to these changes. Laboratory results, with the HWTD, show that small variations in gradation do affect performance and should be considered.

The job mix formula (JMF) and the allowable tolerance limits play an important role in pavement construction and pavement performance. It sets lower and upper boundaries for contractors to get paid for the job and ensures consistency and a minimum level of quality in the finished product. The tolerance bounds can also influence the economics of a specific job. For example, choosing a gradation that is coarser than the target one (JMF) can significantly cut down on the amount of asphalt binder needed for the job and reduce contractor costs. However, this procedure may not necessarily yield the highest quality product. Hence it is important to observe and quantify how small variation within tolerances effects pavement performance. In this study, the researchers focused on the effect on rutting performance, but to do so effectively, other pavement distress such as fatigue cracking must also be observed before the findings of this research could be generalized.

5.1 Future Recommendations

The binder content and aggregate gradation of the asphalt mixture play a significant role in pavement performance. Even small variations of these properties can have pronounced effects on the life of the pavement structure. For example, in this research study it was determined that increasing the binder content from 5.6% to 6.0% for mixture Type D with a fine gradation resulted in a 67% increase in pavement rutting when tested with the HWTD. The major drawback of this study was the lack of volumetric data available for the specific specimens tested under the HWTD. The densities had to be assumed to fall within the testing specification range. To develop a better understanding of how certain volumetric properties effect pavement rutting, it is critical to conduct the HWTD analysis with complete volumetric data of the tested specimens. This would lead to more accurate modeling of pavement sections with the MEPDG and an overall better correlation of results between predictions and laboratory results.

It should also be noted that this research study was conducted only with limestone mixes. Limestone is, in general, softer and more porous than siliceous river gravels also commonly used in Texas. If this research study could be extended to more mixes and more aggregate types, the correlations between the HWTD test results and the MEPDG predictions could be better characterized and more representative.

The current version of the MEPDG does not allow the designer to discern between aggregate types when selecting material characteristics for the analysis. Although the MEPDG does offer three levels of inputs for interpolating the dynamic modulus, two of them (Levels 2 and 3) rely on the revised Witczak equation. The last level of inputs (Level 1) requires a number of sophisticated laboratory tests to calculate the dynamic modulus (NCHRP, 2004).

Since the MEPDG does not discern between aggregate types used in the mixture unless a series of laboratory tests is conducted to determine the dynamic modulus, this can pose a problem for routine design in many highway agencies. The MEPDG may not have the ability to accurately predict pavement rutting for all types of aggregates. Chapter 2 of the Final Report for the *Guide for Mechanistic-Empirical Design of New and Rehabilitate Pavement Structures* mentions that the original Witczak dynamic modulus prediction equation employed by the MEPDG would "loose accuracy for values of the measured dynamic modulus higher than approximately 3 million psi" (NCHRP, 2004). Since then the model has been revised to eliminate bias; nevertheless, it is important to test its integrity against proven performance tests such as the Hamburg Wheel Tracking Device.

REFERENCES

AASHTO 2006a. *Standard Method of Test for Hamburg Wheel-Track Testing of Compacted Hot-Mix Asphalt (HMA)*. AASHTO Designation T324-04. American Association of State Highway and Transportation Officials. Washington D.C.

AASHTO 2006b. *Bending Beam Fatigue Test*. AASHTO Designation T321-03. American Association of State Highway and Transportation Officials. Washington D.C.

AASHTO 2008. Mechanistic-Empirical Pavement Design Guide, *A Manual of Practice*. American Association of State Highway and Transportation Officials, Washington D.C., July 2008.

Banerjee, Ambarish., Aguiar-Moya, J. P., Prozzi, J. A. (2009). *Texas Experience using LTPP for Calibration of the MEPDG Permanent Deformation Models*. TRB Paper 09-0829, Transportation Research Board, Washington D.C., 2009.

Brown, E. R., Khandal, P.S. and Zhang, J. 2001. *Performance Testing for Hot Mix Asphalt*, NCAT Report 01-05, National Center for Asphalt Technology, Auburn, Alabama.

Huang, Yang H. *Pavement Analysis and Design.* Pearson Prentice Hall, Upper Saddle River, NJ, 2004.

Mamlouk, Michael S., Zaniewski, John P. *Materials for Civil and Construction Engineers: Second Edition*. Pearson Prentice Hall, Upper Saddle River, NJ, 2006.

NCHRP 2003. Research Results Digest, No. 284: *Refining the Calibration and Validation of Hot Mix Asphalt Performance Models: An Experimental Plan and Database*, Transportation Research Board of the National Academies, Washington, DC, 2003.

NCHRP 2004. *Guide for Mechanistic-Empirical Design of New and Rehabilitated Pavement Structures Final Report: Part 2 Design Inputs*. NCHRP 1-37A. National Cooperative Highway Research Program, Washington D.C. March 2004.

Prozzi, J.A., Aguiar-Moya, J.P., Smit, A.F., Tahmoressi, M., and Fults, K., (2006). *Recommendations for Reducing Superpave Compaction Effort to Improve Mixture Durability and Fatigue Performance.* CTR Technical Report No: 0-5132-1, Center for Transportation Research, The University of Texas at Austin. Austin, TX, October 2006.

Texas Department of Transportation. Test Procedures, *200-F Bituminous Test Procedures: Tex-204-F, Design of Bituminous Mixtures*, http://www.txdot.gov/business/contractors_consultants/test_procedures/default.htm. Accessed March, 2009.

Texas Department of Transportation. Test Procedures, *200-F, Bituminous Test Procedures: Tex 242-F Hamburg Wheel Tracking Device Test*, http://www.txdot.gov/business/contractors_consultants/ test_procedures/default.htm. Accessed March, 2009.

Texas Department of Transportation. Test Procedures, *200-F, Bituminous Test Procedures: Tex-248-F The Overlay Test*, http://www.txdot.gov/business/contractors_consultants/ test_procedures/default.htm
Accessed March, 2009.

Texas Department of Transportation. *Standard Specifications for Construction and Maintenance of Highways, Streets, and Bridges,* Texas Department of Transportation, Austin, TX, 2004.

Yildirim, Yetkin., Stokoe II, Kenneth H., (2006). *Analysis of Hamburg Wheel Tracking Device Results in Relation to Field Performance.* TXDOT Project No. 0-4185, Center for Transportation Research. The University of Texas at Austin. Austin, TX, November 2006.

APPENDIX A: Calculating the Lower Bound Average for HWTD Analysis

The lower bound average was the statistic chosen for calculating deformation in specimens under the HWTD. Due to the high sensitivity of the LVDT devices used to capture deformation, the lower bound average was determined to be the most logical approach because it significantly reduced noise and allowed for a continuous deformation curve which decreased over time. To apply this technique, several steps were taken in the following order:

1. Observe the deformation at points 5, 6, and 7 for each record.
2. Obtain the average deformation from points 5, 6, and 7 for each record.
3. If the average deformation recorded at per se point *a* was greater than the average deformation recorded at per se point *b*, use the average deformation at point *a* as the lower bound average until a greater average deformation is found in a preceding record.
4. If the average deformation recorded at point *a* was smaller than the average deformation recorded at point *b*, then use the average deformation at point *b* as the lower bound average until a greater average deformation is found in a preceding record.

APPENDIX B: Calculating the Slope Parameter for HWTD Analysis

The performance of an asphalt mix measured by the HWTD can be split into several parts: the post compaction point, the creep slope, the stripping inflection point and the stripping slope. The creep slope, which indicates rutting susceptibility, can be calculated by drawing a line that best fits the deformation curve from the postcompaction point to the stripping inflection point (Prozzi, Aguiar-Moya, Smit, Tahmoressi, and Fults, 2006).

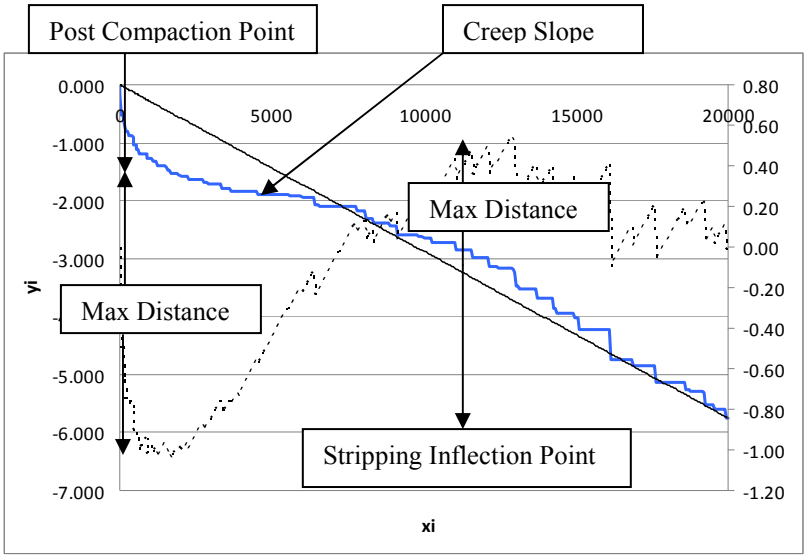

Figure B.1. Concept of Differences Approach to Determine Slope

The creep slope can be determined by first defining a straight line from the initial response value (x_i,y_i) to the final response value (x_f,y_f). Then the difference between this defined line and the performance curve can be calculated (y-ý) and the points where the differences are at a maximum or a minimum can be defined as the postcompaction point and the stripping inflection point. Having defined these two points, a simple regression can be performed to define the creep slope which is the line between these two points.

In some instances, the performance data might not have a stripping inflection point because the specimen did not reach a point of moisture susceptibility at the conclusion of the test (20,000 wheel passes). In such an instance the last point is still considered to be on the creep slope line and is used to calculate the z-slope.

The creep (Z) slope analysis was conducted for all specimens tested with the HWTD and the results can be found in Appendix E.

APPENDIX C: Volumetric Data Used to Model Sections in the MEPDG

	Pb	Gradation	Gmm_{theo}	VTM	Gmb	UW	Vabs	VMA	VEFF
C001	4.60%	Target	2.43	7.00%	2.26	140.77	1.50%	15.57%	8.57%
				6.00%	2.28	142.28	1.50%	14.68%	8.68%
				8.00%	2.23	139.25	1.50%	16.47%	8.47%
C002	4.30%	Target	2.44	7.00%	2.27	141.37	1.50%	14.96%	7.96%
				6.00%	2.29	142.89	1.50%	14.06%	8.06%
				8.00%	2.24	139.85	1.50%	15.86%	7.86%
C003	4.00%	Target	2.45	7.00%	2.28	141.98	1.50%	14.34%	7.34%
				6.00%	2.30	143.50	1.50%	13.43%	7.43%
				8.00%	2.25	140.45	1.50%	15.24%	7.24%
C004	5.00%	Target	2.41	7.00%	2.24	139.97	1.50%	16.39%	9.39%
				6.00%	2.27	141.48	1.50%	15.51%	9.51%
				8.00%	2.22	138.47	1.50%	17.27%	9.27%
C005	5.00%	Fine	2.43	7.00%	2.26	140.82	1.50%	16.45%	9.45%
				6.00%	2.28	142.33	1.50%	15.57%	9.57%
				8.00%	2.23	139.30	1.50%	17.34%	9.34%
C006	4.60%	Fine	2.44	7.00%	2.27	141.62	1.50%	15.64%	8.64%
				6.00%	2.29	143.15	1.50%	14.75%	8.75%
				8.00%	2.25	140.10	1.50%	16.53%	8.53%
C007	4.30%	Fine	2.45	7.00%	2.28	142.24	1.50%	15.02%	8.02%
				6.00%	2.30	143.77	1.50%	14.12%	8.12%
				8.00%	2.25	140.71	1.50%	15.91%	7.91%
C008	4.00%	Fine	2.46	7.00%	2.29	142.85	1.50%	14.39%	7.39%
				6.00%	2.31	144.39	1.50%	13.49%	7.49%
				8.00%	2.26	141.32	1.50%	15.30%	7.30%
C009	5.00%	Coarse	2.42	7.00%	2.25	140.52	1.50%	16.43%	9.43%
				6.00%	2.28	142.03	1.50%	15.55%	9.55%
				8.00%	2.23	139.01	1.50%	17.31%	9.31%
C010	4.60%	Coarse	2.44	7.00%	2.26	141.32	1.50%	15.61%	8.61%
				6.00%	2.29	142.84	1.50%	14.72%	8.72%
				8.00%	2.24	139.80	1.50%	16.51%	8.51%
C011	4.30%	Coarse	2.44	7.00%	2.26	141.32	1.50%	14.95%	7.95%
				6.00%	2.29	142.84	1.50%	14.06%	8.06%
				8.00%	2.24	139.80	1.50%	15.85%	7.85%
C012	4.00%	Coarse	2.46	7.00%	2.28	142.54	1.50%	14.37%	7.37%
				6.00%	2.31	144.08	1.50%	13.47%	7.47%
				8.00%	2.26	141.01	1.50%	15.28%	7.28%

	Pb	Gradation	Gmm_{theo}	VTM	Gmb	UW	Vabs	VMA	VEFF
D001	5.30%	Target	2.40	7.00%	2.24	139.51	1.50%	17.00%	10.00%
				6.00%	2.26	141.01	1.50%	16.13%	10.13%
				8.00%	2.21	138.01	1.50%	17.88%	9.88%
D002	5.00%	Target	2.41	7.00%	2.25	140.10	1.50%	16.40%	9.40%
				6.00%	2.27	141.61	1.50%	15.52%	9.52%
				8.00%	2.22	138.59	1.50%	17.28%	9.28%
D003	4.60%	Target	2.43	7.00%	2.26	140.90	1.50%	15.58%	8.58%
				6.00%	2.28	142.41	1.50%	14.69%	8.69%
				8.00%	2.23	139.38	1.50%	16.48%	8.48%
D004	5.60%	Target	2.39	7.00%	2.23	138.92	1.50%	17.60%	10.60%
				6.00%	2.25	140.42	1.50%	16.73%	10.73%
				8.00%	2.20	137.43	1.50%	18.47%	10.47%
D005	4.60%	Coarse	2.43	7.00%	2.26	141.24	1.50%	15.61%	8.61%
				6.00%	2.29	142.76	1.50%	14.72%	8.72%
				8.00%	2.24	139.72	1.50%	16.50%	8.50%
D006	5.00%	Coarse	2.42	7.00%	2.25	140.44	1.50%	16.43%	9.43%
				6.00%	2.27	141.95	1.50%	15.54%	9.54%
				8.00%	2.23	138.93	1.50%	17.31%	9.31%
D007	5.30%	Coarse	2.41	7.00%	2.24	139.84	1.50%	17.03%	10.03%
				6.00%	2.27	141.34	1.50%	16.16%	10.16%
				8.00%	2.22	138.34	1.50%	17.91%	9.91%
D008	5.60%	Coarse	2.40	7.00%	2.23	139.25	1.50%	17.63%	10.63%
				6.00%	2.26	140.75	1.50%	16.76%	10.76%
				8.00%	2.21	137.75	1.50%	18.50%	10.50%
D009	5.30%	Fine	2.41	7.00%	2.25	140.11	1.50%	17.05%	10.05%
				6.00%	2.27	141.62	1.50%	16.18%	10.18%
				8.00%	2.22	138.61	1.50%	17.93%	9.93%
D010	5.60%	Fine	2.40	7.00%	2.24	139.52	1.50%	17.66%	10.66%
				6.00%	2.26	141.02	1.50%	16.79%	10.79%
				8.00%	2.21	138.02	1.50%	18.53%	10.53%
D011	5.00%	Fine	2.40	7.00%	2.24	139.52	1.50%	16.35%	9.35%
				6.00%	2.26	141.02	1.50%	15.47%	9.47%
				8.00%	2.21	138.02	1.50%	17.24%	9.24%
D012	6.00%	Fine	2.39	7.00%	2.22	138.74	1.50%	18.45%	11.45%
				6.00%	2.25	140.23	1.50%	17.59%	11.59%
				8.00%	2.20	137.24	1.50%	19.31%	11.31%

	Pb	Gradation	Gmm_{theo}	VTM	Gmb	UW	Vabs	VMA	VEFF
SD01	6.20%	Target	2.36	7.00%	2.20	136.99	1.50%	18.72%	11.72%
				6.00%	2.22	138.47	1.50%	17.86%	11.86%
				8.00%	2.17	135.52	1.50%	19.57%	11.57%
SD02	5.70%	Target	2.38	7.00%	2.21	137.94	1.50%	17.73%	10.73%
				6.00%	2.23	139.43	1.50%	16.87%	10.87%
				8.00%	2.19	136.46	1.50%	18.60%	10.60%
SD03	6.50%	Target	2.35	7.00%	2.19	136.43	1.50%	19.30%	12.30%
				6.00%	2.21	137.90	1.50%	18.45%	12.45%
				8.00%	2.16	134.96	1.50%	20.15%	12.15%
SD04	6.50%	Fine	2.35	7.00%	2.19	136.42	1.50%	19.30%	12.30%
				6.00%	2.21	137.89	1.50%	18.45%	12.45%
				8.00%	2.16	134.96	1.50%	20.15%	12.15%
SD05	6.20%	Fine	2.36	7.00%	2.20	136.99	1.50%	18.71%	11.71%
				6.00%	2.22	138.46	1.50%	17.86%	11.86%
				8.00%	2.17	135.51	1.50%	19.57%	11.57%
SD06	5.70%	Fine	2.38	7.00%	2.21	137.94	1.50%	17.73%	10.73%
				6.00%	2.23	139.42	1.50%	16.86%	10.86%
				8.00%	2.19	136.45	1.50%	18.60%	10.60%
SD07	6.50%	Coarse	2.34	7.00%	2.18	135.92	1.50%	19.25%	12.25%
				6.00%	2.20	137.38	1.50%	18.39%	12.39%
				8.00%	2.15	134.46	1.50%	20.10%	12.10%
SD08	6.20%	Coarse	2.35	7.00%	2.19	136.48	1.50%	18.67%	11.67%
				6.00%	2.21	137.95	1.50%	17.81%	11.81%
				8.00%	2.16	135.01	1.50%	19.52%	11.52%
SD09	5.70%	Coarse	2.37	7.00%	2.20	137.42	1.50%	17.69%	10.69%
				6.00%	2.23	138.90	1.50%	16.82%	10.82%
				8.00%	2.18	135.94	1.50%	18.56%	10.56%

APPENDIX D: MEPDG Results for Modeled Sections

Type C MEPDG Rutting Results (by month)									
	1	**3**	**6**	**12**	**36**	**60**	**120**	**180**	**240**
C001	0.014	0.017	0.017	0.043	0.068	0.088	0.128	0.162	0.193
	0.013	0.016	0.016	0.04	0.064	0.083	0.12	0.151	0.181
	0.015	0.018	0.019	0.046	0.074	0.096	0.138	0.175	0.209
C002	0.013	0.016	0.017	0.041	0.066	0.085	0.123	0.156	0.186
	0.012	0.015	0.016	0.038	0.062	0.08	0.115	0.146	0.174
	0.015	0.018	0.018	0.044	0.071	0.092	0.133	0.168	0.201
C003	0.013	0.016	0.016	0.039	0.063	0.082	0.118	0.149	0.178
	0.012	0.014	0.015	0.037	0.059	0.077	0.111	0.14	0.167
	0.014	0.017	0.017	0.042	0.068	0.088	0.127	0.161	0.192
C004	0.015	0.018	0.018	0.045	0.072	0.093	0.134	0.17	0.203
	0.014	0.017	0.017	0.042	0.067	0.087	0.125	0.159	0.189
	0.016	0.019	0.02	0.049	0.078	0.101	0.145	0.184	0.219
C005	0.014	0.017	0.018	0.044	0.07	0.091	0.131	0.166	0.198
	0.013	0.016	0.017	0.041	0.065	0.084	0.122	0.155	0.185
	0.015	0.019	0.019	0.047	0.076	0.098	0.141	0.179	0.214
C006	0.014	0.017	0.017	0.042	0.067	0.086	0.125	0.158	0.189
	0.013	0.015	0.016	0.039	0.063	0.081	0.117	0.148	0.177
	0.015	0.018	0.018	0.045	0.072	0.093	0.135	0.171	0.204
C007	0.013	0.016	0.016	0.04	0.064	0.083	0.12	0.152	0.182
	0.012	0.015	0.015	0.037	0.06	0.078	0.113	0.142	0.17
	0.014	0.017	0.018	0.043	0.069	0.089	0.13	0.164	0.196
C008	0.013	0.015	0.016	0.038	0.062	0.08	0.115	0.146	0.174
	0.012	0.014	0.015	0.036	0.057	0.075	0.108	0.137	0.163
	0.014	0.016	0.017	0.041	0.066	0.086	0.124	0.157	0.188
C009	0.015	0.018	0.019	0.047	0.074	0.096	0.139	0.175	0.21
	0.014	0.017	0.018	0.043	0.069	0.09	0.13	0.164	0.196
	0.016	0.02	0.02	0.05	0.08	0.104	0.15	0.19	0.227
C010	0.015	0.018	0.018	0.044	0.071	0.092	0.133	0.168	0.2
	0.013	0.016	0.017	0.041	0.066	0.085	0.124	0.156	0.187
	0.016	0.019	0.019	0.048	0.077	0.099	0.143	0.181	0.216
C011	0.014	0.017	0.017	0.042	0.068	0.088	0.127	0.161	0.192
	0.013	0.016	0.016	0.04	0.064	0.082	0.119	0.15	0.18
	0.015	0.018	0.019	0.046	0.073	0.095	0.137	0.173	0.207
C012	0.013	0.016	0.017	0.041	0.065	0.084	0.122	0.154	0.185
	0.012	0.015	0.015	0.038	0.061	0.079	0.114	0.144	0.173
	0.014	0.018	0.018	0.044	0.07	0.091	0.132	0.167	0.199

Type D MEPDG Rutting Results (by month)									
	1	**3**	**6**	**12**	**36**	**60**	**120**	**180**	**240**
D001	0.018	0.022	0.022	0.054	0.086	0.112	0.161	0.205	0.245
	0.017	0.02	0.021	0.051	0.08	0.104	0.15	0.191	0.228
	0.019	0.023	0.024	0.059	0.094	0.121	0.175	0.221	0.265
D002	0.017	0.021	0.021	0.053	0.084	0.108	0.156	0.198	0.237
	0.016	0.019	0.02	0.049	0.078	0.101	0.146	0.185	0.221
	0.019	0.023	0.023	0.057	0.09	0.117	0.169	0.214	0.256
D003	0.016	0.02	0.02	0.05	0.08	0.103	0.149	0.189	0.226
	0.015	0.018	0.019	0.047	0.075	0.097	0.139	0.177	0.211
	0.018	0.022	0.022	0.054	0.086	0.112	0.161	0.204	0.244
D004	0.018	0.022	0.023	0.056	0.089	0.115	0.166	0.211	0.252
	0.017	0.021	0.021	0.052	0.083	0.107	0.155	0.196	0.235
	0.02	0.024	0.025	0.061	0.097	0.125	0.18	0.228	0.273
D005	0.018	0.021	0.022	0.054	0.085	0.11	0.159	0.202	0.241
	0.016	0.02	0.02	0.05	0.08	0.103	0.149	0.189	0.226
	0.019	0.023	0.024	0.058	0.092	0.119	0.172	0.218	0.261
D006	0.018	0.022	0.023	0.056	0.089	0.116	0.167	0.212	0.253
	0.017	0.021	0.021	0.052	0.083	0.108	0.156	0.198	0.236
	0.02	0.024	0.025	0.061	0.097	0.125	0.18	0.229	0.274
D007	0.019	0.023	0.024	0.058	0.092	0.12	0.172	0.218	0.261
	0.018	0.021	0.022	0.054	0.086	0.111	0.16	0.204	0.244
	0.021	0.025	0.026	0.063	0.1	0.129	0.187	0.236	0.283
D008	0.02	0.024	0.025	0.06	0.095	0.123	0.177	0.225	0.269
	0.018	0.022	0.023	0.056	0.089	0.114	0.165	0.209	0.251
	0.021	0.026	0.027	0.065	0.103	0.134	0.193	0.244	0.292
D009	0.016	0.019	0.02	0.049	0.077	0.1	0.145	0.184	0.22
	0.015	0.018	0.018	0.045	0.072	0.094	0.135	0.171	0.205
	0.017	0.021	0.021	0.053	0.084	0.109	0.157	0.199	0.238
D010	0.016	0.02	0.02	0.05	0.08	0.103	0.149	0.19	0.227
	0.015	0.018	0.019	0.047	0.074	0.096	0.139	0.177	0.211
	0.018	0.022	0.022	0.055	0.087	0.112	0.162	0.205	0.246
D011	0.015	0.019	0.019	0.047	0.075	0.097	0.14	0.177	0.212
	0.014	0.017	0.018	0.044	0.07	0.09	0.131	0.166	0.198
	0.017	0.02	0.021	0.051	0.081	0.105	0.151	0.192	0.229
D012	0.017	0.021	0.021	0.052	0.083	0.107	0.155	0.197	0.235
	0.016	0.019	0.02	0.048	0.077	0.1	0.144	0.183	0.218
	0.018	0.023	0.023	0.057	0.09	0.116	0.168	0.213	0.255

SMA D MEPDG Rutting Results (by month)									
	1	**3**	**6**	**12**	**36**	**60**	**120**	**180**	**240**
SD01	0.019	0.023	0.024	0.058	0.092	0.119	0.172	0.218	0.261
	0.018	0.021	0.022	0.054	0.085	0.111	0.16	0.203	0.242
	0.021	0.025	0.026	0.063	0.1	0.129	0.187	0.236	0.283
SD02	0.018	0.022	0.023	0.056	0.088	0.114	0.165	0.209	0.25
	0.017	0.02	0.021	0.052	0.082	0.106	0.153	0.194	0.232
	0.02	0.024	0.025	0.06	0.095	0.124	0.178	0.226	0.27
SD03	0.02	0.024	0.024	0.06	0.094	0.122	0.176	0.223	0.267
	0.018	0.022	0.022	0.055	0.088	0.114	0.164	0.208	0.248
	0.021	0.026	0.026	0.065	0.103	0.133	0.191	0.242	0.29
SD04	0.019	0.023	0.024	0.059	0.093	0.12	0.173	0.22	0.263
	0.018	0.022	0.022	0.054	0.086	0.112	0.161	0.204	0.244
	0.021	0.025	0.026	0.064	0.101	0.13	0.188	0.238	0.285
SD05	0.019	0.023	0.023	0.057	0.091	0.117	0.169	0.214	0.256
	0.017	0.021	0.022	0.053	0.084	0.109	0.157	0.2	0.238
	0.02	0.025	0.025	0.062	0.098	0.127	0.183	0.232	0.278
SD06	0.018	0.022	0.022	0.055	0.087	0.112	0.162	0.205	0.246
	0.017	0.02	0.021	0.051	0.081	0.104	0.15	0.191	0.228
	0.019	0.024	0.024	0.059	0.094	0.121	0.175	0.222	0.266
SD07	0.02	0.025	0.025	0.062	0.098	0.127	0.183	0.231	0.277
	0.019	0.023	0.023	0.057	0.091	0.117	0.169	0.215	0.257
	0.022	0.027	0.027	0.067	0.106	0.137	0.198	0.251	0.3
SD08	0.02	0.024	0.025	0.06	0.095	0.123	0.178	0.226	0.27
	0.018	0.022	0.023	0.056	0.089	0.115	0.166	0.21	0.251
	0.021	0.026	0.027	0.065	0.104	0.134	0.193	0.245	0.292
SD09	0.019	0.023	0.023	0.058	0.091	0.118	0.17	0.216	0.258
	0.017	0.021	0.022	0.054	0.085	0.11	0.159	0.201	0.24
	0.02	0.025	0.025	0.063	0.099	0.128	0.185	0.234	0.28

APPENDIX E: HWTD Results for Compacted Specimens

HWTD		Maximum Deformation		10,000	15,000	20,000	
	Pb	Max Cycles	Deformation (in.)	|Deformation (in)|			Slope
C001	4.00%	20,000	0.1683	0.0844	0.1184	0.1683	-0.00025
C002	4.30%	20,000	0.2264	0.1040	0.1579	0.2264	-0.00014
C003	4.60%	20,000	0.2215	0.1201	0.1737	0.2215	-9.30E-05
C004	5.00%	20,000	0.3542	0.2049	0.2997	0.3542	-0.00038
C005	4.00%	20,000	0.0995	0.0596	0.0708	0.0995	-0.00013
C006	4.30%	20,000	0.1208	0.0675	0.0836	0.1208	-0.00039
C007	4.60%	20,000	0.3329	0.1474	0.2380	0.3329	-9.50E-05
C008	5.00%	20,000	0.1689	0.1100	0.1351	0.1689	-6.00E-05
C009	4.00%	20,000	0.1813	0.0824	0.1418	0.1813	-0.00019
C010	4.30%	20,000	0.1807	0.1030	0.1337	0.1807	-0.00017
C011	4.60%	20,000	0.1810	0.1031	0.1340	0.1810	-0.00015
C012	5.00%	20,000	0.2031	0.1125	0.1443	0.2031	-0.00018
D001	4.60%	20,000	0.1486	0.0791	0.1110	0.1486	-0.0002
D002	4.60%	20,000	0.1568	0.1149	0.1404	0.1568	-0.00016
D003	5.00%	20,000	0.1625	0.0830	0.1257	0.1625	-0.00014
D004	5.00%	20,000	0.1511	0.1233	0.1236	0.1511	-0.00016
D005	5.00%	20,000	0.3248	0.1564	0.2099	0.3248	-0.00013
D006	5.30%	20,000	0.2175	0.1139	0.1670	0.2175	-0.00011
D007	5.30%	20,000	0.2882	0.1681	0.2185	0.2882	-0.00027
D008	5.30%	20,000	0.3469	0.2333	0.2751	0.3469	-0.00015
D009	5.60%	20,000	0.2226	0.1503	0.1883	0.2226	-0.00031
D010	5.60%	20,000	0.2060	0.1506	0.1566	0.2060	-0.00037
D011	5.60%	20,000	0.4168	0.2416	0.3246	0.4168	-0.00015
D012	6.00%	11,629	0.5203	0.5793	0.5212	--	-0.00117
SD01	6.20%	20,000	0.3691	0.2945	0.3293	0.3691	-0.0002
SD02	5.70%	20,000	0.2976	0.2461	0.2676	0.2976	-0.00017
SD03	6.50%	20,000	0.4439	0.3350	0.3935	0.4439	-0.00029
SD04	6.50%	20,000	0.5544	0.4485	0.4925	0.5544	-0.00033
SD05	6.20%	20,000	0.3676	0.3207	0.3408	0.3676	-0.00016
SD06	5.70%	20,000	0.4043	0.3269	0.3690	0.4043	-0.00021
SD07	6.50%	20,000	0.4143	0.3445	0.3714	0.4143	-0.0002
SD08	6.20%	20,000	0.3874	0.3547	0.3617	0.3874	-0.00013
SD09	5.70%	20,000	0.2704	0.2423	0.2626	0.2704	-0.00011